Nickel Hydrides Supported by a Non-Innocent Diphosphine Arene Pincer: Mechanistic Studies of Nickel-Arene H-Migration and Partial Arene Hydrogenation

Sibo Lin, Michael W. Day and Theodor Agapie*

Department of Chemistry and Chemical Engineering, California Institute of Technology, 1200 E. California Blvd. MC 127-72, Pasadena, CA, USA

Supporting Information

Experimental Details

General Considerations. All air- and moisture-sensitive compounds were manipulated using standard vacuum line, Schlenk, or cannula techniques or in a glove box under a nitrogen atmosphere. Compounds **1, 4** [2,2"-bis(diisopropylphosphino)terphenyl], and $[H(OEt_2)_2][B(C_6H_3(CF_3)_2)_4]$ (Brookhart's acid) were synthesized as previously reported.[1,2] Solvents for air- and moisture-sensitive reactions were dried over sodium benzophenone ketyl, calcium hydride, or by the method of Grubbs.[3] Acetonitrile-d_3 and dichloromethane-d_2, were purchased from Cambridge Isotope Laboratories (CIL) and vacuum transferred from calcium hydride. Benzene-d_6 was also purchased from CIL and vacuum transferred from sodium benzophenone ketyl. Other materials were used as received. ^{1}H, ^{13}C, and ^{31}P NMR spectra were recorded on Varian Mercury spectrometers at room temperature, unless indicated otherwise. ^{1}H and ^{13}C NMR chemical shifts are reported relative to residual solvent.[4] ^{31}P NMR chemical shifts are reported with respect to the instrument solvent lock when a deuterated solvent was used. Gas chromatography-mass spectrometry (GC-MS) analysis was performed upon filtering the sample through a plug of silica gel. Fast atom bombardment-mass spectrometry (FAB-MS) analysis was performed with a JEOL JMS-600H high resolution mass spectrometer. Elemental analysis was conducted by Midwest Microlab, LLC (Indianapolis, IN).

Synthesis of 2.

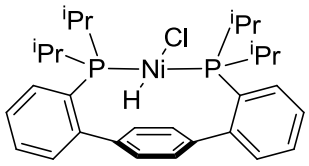

2

A Schlenk flask was charged with **1** (650 mg, 1.25 mmol) and 30 mL of Et_2O. A syringe was used to add 0.69 mL of 2.0 M HCl/Et_2O (1.37 mmol) to the reaction, which changed from dark red to orange color in seconds. After 30 minutes, the reaction was concentrated to a powder and sequentially washed and filtered with 10 mL of hexanes, Et_2O, and toluene. The product was obtained by concentration of the toluene fraction to a light orange powder (470 mg, 0.84 mmol, 67%), which was pure by NMR spectroscopy. Orange XRD-quality crystals were grown by layering pentane on a toluene solution of the product for 2 days at room temperature. ^{1}H NMR (300 MHz, C_6D_6) δ 8.44 (s, 2H, central aryl-*H*, $^1J_{CH}$ = 172.8 Hz), 7.47 (app d, 2H, aryl-*H*), 7.22 (m, 4H, aryl-*H*), 7.09 (m, 2H, aryl-*H*), 6.93 (s, 2H, central aryl-*H*, $^1J_{CH}$ = 161.6 Hz), 2.68 (br m, 2H, C*H*$(CH_3)_2$), 1.63 (m, 14H, C*H*$(CH_3)_2$ and 2[CH(C*H*$_3)_2$]), 0.92 (app dd, 6H, CH(C*H*$_3)_2$), 0.48 (app dd, 6H, CH(C*H*$_3)_2$), -28.97 (t, J_{P-H} = 79.0 Hz, 1H, Ni-*H*). ^{13}C{^{1}H} NMR (101 MHz, C_6D_6) δ: 150.15 (t, J = 6.7 Hz), 137.15 (app t), 131.77 (s), 130.78 (t, J = 16.1 Hz), 129.66 (s), 126.88 (s), 121.86 (s), 29.33 (br t), 26.56 (br t), 19.59 (s), 19.37 (s), 19.00 (s), 17.78 (s). ^{31}P{^{1}H} NMR (121 MHz, C_6D_6) δ: 23.4 (dd, J_{P-H} = 74.7 Hz, J_{P-P} = 5.3 Hz). Anal. Calcd. for $C_{30}H_{41}ClNiP_2$ (%): C, 64.60; H, 7.41. Found: C, 63.91; H, 7.26. MS (m/z): calcd, 556.1726 (M^+); found 556.1750 (FAB-MS, M^+). λ_{max} (benzene, nm), ε (M^{-1} cm^{-1}): 322, 6.36 x 10^2; 425, 1.72 x 10^2.

Conversion of 2 to 3 and 4.

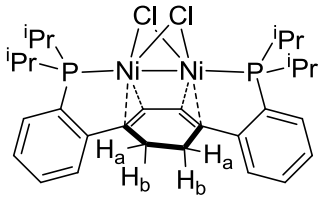

3

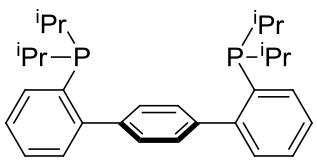

4

A stock solution of **2** (32.6 mg, 0.058 mmol) in 1.6 mL d_8-toluene was prepared. A J. Young NMR tube was charged with 0.5 mL of this 36.5 mM stock solution. The complete conversion of **2** to **3** (0.5 equiv.) and **4 (**0.5 equiv.) was observed

over 3h in an NMR spectrometer that was preequilibrated to 90 °C. The two products were separated by removing volatiles under vacuum and washing the resultant powder with hexanes. **4** dissolves in hexanes, leaving mostly **3**. Dark puple XRD-quality crystals of **3** could be isolated by vapor diffusion of pentane into a toluene solution of **3** (5.0 mg, 0.009 mmol, 84% yield). ^{1}H NMR (300 MHz, C_6D_6) δ 7.40 (app d, 2H, aryl-*H*), 7.05 (app t, 2H, aryl-*H*), 6.96 (app t, 2H, aryl-*H*), 6.80 (m, 2H, aryl-*H*), 4.64 (s, 2H, olefin-*H*), 2.30 (d, J = 11.4 Hz, 2H, CH_aH), 1.94 (m, 2H, CH(CH_3)$_2$), 1.79 (d, J = 11.4 Hz, 2H, CHH_b), 1.63 (m, 2H, CH(CH_3)$_2$), 1.32 (m, 12H, CH(CH_3)$_2$), 0.96 (m, 12H, CH(CH_3)$_2$). ^{31}P NMR (121 MHz, C_6D_6) δ: 52.7. MS (m/z): calcd, 652.0816 (M^+); found 652.0827 (FAB-MS, M^+). λ_{max} (benzene, nm), ε (M^{-1} cm^{-1}): 327, 1.71 x 10^3; 392, 5.78 x 10^2; 508, 4.25 x 10^2; 670, 8.44 x 10^1.

A 1D NOE experiment showed interaction between the aliphatic peak at 1.79 ppm and an aromatic peak at 7.40 ppm. Thus, based on H—H distances observed in the XRD-derived structure, that peak was assigned to the H_b *(exo*) protons of the central ring; the peak at 2.30 ppm did not exhibit 1D NOE cross-peaks with aromatic protons and was assigned to the H_a (*endo*) protons of the central ring. (See Figure S8).

Synthesis of 1,4-diiodo-2,3,5,6-tetradeuterobenzene. This synthesis was adapted from a literature procedure.[5] An oven-dried three-necked flask was charged with $NaIO_4$ (3.050 g, 14.26 mmol), freshly ground I_2 (10.85 g, 42.78 mmol), AcOH (50 mL), and Ac_2O (25 mL) under a counterflow of nitrogen. A thermometer was inserted through a septum such that the tip was submerged in the reaction, taking care to not interfere with the stir bar. Subsequent temperature measurements were taken using this thermometer. The red suspension was chilled to 5-10 °C using an ice water bath. With vigorous stirring, H_2SO_4 (13.3 mL) was added dropwise slowly enough to keep the temperature between 5-10 °C. Dry C_6D_6 (3.17 mL, 35.65 mmol) was added, and the reaction was allowed to reach room temperature. Reaction progress was monitored by GC-MS over 4h. The reaction was quenched by pouring a solution of Na_2SO_3 (20g in 1 L H_2O) into the reaction flask. The crude was filtered and washed with H_2O and then Et_2O to yield a white solid, the purity of which was checked by TLC and identified by GC-MS as the desired product (7.12 g, 21.3 mmol, 60%) MS (m/z): calcd, 333.8653 (M^+); found 334 (GC-MS, M^+).

Synthesis of 4-d$_4$. 4-*d*$_4$ was synthesized with 1,4-diiodo-2,3,5,6-tetradeuterobenzene as **4** was previously synthesized with 1,4-diiodobenzene.[1] The ^{1}H and ^{31}P NMR spectra match those of **4**, except that no ^{1}H signal was detected on the central arene (7.55 ppm, see Figure S1).

Synthesis of 1-d$_4$. 1-*d*$_4$ was synthesized with **4-*d*$_4$** as **1** was previously synthesized with **4**.[1] The ^{1}H and ^{31}P NMR spectra match those of **1**, except that no ^{1}H signal was detected on the central arene (5.52 ppm, see Figure S2).

Synthesis of 2-d$_4$. 2-*d*$_4$ was synthesized with **1-*d*$_4$** as **2** was previously synthesized with **1** (vide supra). The ^{1}H and ^{31}P NMR spectra match those of **2**, except that less than 4% ^{1}H signal was detected on the central arene (8.44, 6.93 ppm, see Figure S3).

Thermal conversion of 2-*d*$_4$ to partially deuterated 3 and 4. A stock solution of **2-*d*$_4$** (20.0 mg, 0.0356 mmol) in toluene (1.6 mL) was prepared. A J. Young NMR tube was charged with 0.5 mL of this 22.2 mM solution and suspended in a preheated 90 °C oil bath for 3 hours. The complete conversion of **2** to **3** (ca. 0.5 equiv.) and **4** (ca. 0.5 equiv.) was confirmed by ^{31}P NMR. (Attempts to perform this reaction in d_8-toluene and track the deuterium distribution by ^{1}H NMR in the J Young tube were precluded by overlapping peaks between the products and residual protic toluene.) The two products were separated by removing volatiles under vacuum and washing the resultant powder with hexanes. ^{1}H NMR spectroscopy (600MHz, C_6D_6) of the hexanes-soluble materials showed 1 peak with diminished integration relative to **4** (d_0). Assigning the multiplet at 6.95 ppm an integration value of 2 showed that the peak at 7.35 ppm integrated to 0.49 instead of 4. Likewise, ^{1}H NMR spectroscopy of the hexanes-insoluble materials showed 3 peaks with diminished integration relative to **3** (d_0). Assigning the multiplet at 1.63 ppm an integration value of 2 showed that the peaks at 4.64, 2.30, and 1.79 ppm integrated to 0.24, 0.60, and 0.70 respectively, instead of 2.

Synthesis of 5·OTf and 5-NCMe·OTf.

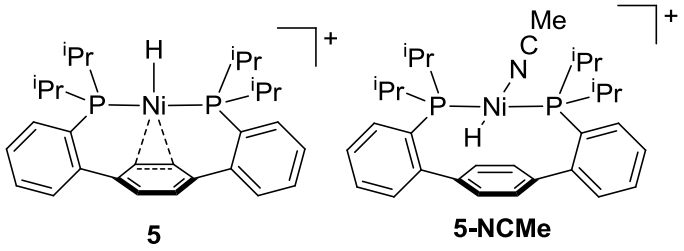

5 **5-NCMe**

To an orange suspension of **2** (107.9 mg, 0.193 mmol) in MeCN (5 mL) was added a solution of TlOTf (68.4 mg, 0.193 mmol) in MeCN (5 mL). In minutes, the reaction was light yellow in color and white powder had precipitated out of solution. The reaction was filtered through a plug of Celite, and volatiles were removed under vacuum to yield spectroscopically pure product as a light yellow powder. Yellow XRD-quality crystals were grown by layering a MeCN solution of the product over Et_2O and storing the layered solution at -35 °C overnight. Prior to elemental analysis and mass spectrometry, these crystals were crushed to a powder and left under vacuum for 3h (94.5 mg, 0.141 mmol, 73% yield). Via XRD, the crystal was determined to have an asymmetric unit consisting of one molecule each of **5·OTf** and **5-NCMe·OTf**. ^{1}H NMR (300 MHz, CD_3CN) δ: 7.79 – 7.70 (m, 4H, aryl-*H*), 7.66 (app t, 2H, aryl-*H*), 7.56 (app t, 2H, aryl-*H)*, 7.38, (br s, 4H, central aryl-*H*, $^1J_{CH}$ = 161.4 Hz), 2.41 (m, 4H, C*H*$(CH_3)_2$), 1.10 (app dd, 12H, CH(C*H*$_3)_2$), 0.93 (app dd, 12H, CH(C*H*$_3)_2$), -25.12 (t, $J_{P\text{-}H}$ = 67.9 Hz, 1H, Ni-*H*). ^{31}P NMR (121 MHz, CD_3CN) δ: 35.56 (app m). ^{13}C{^{1}H} NMR (151 MHz, CD_3CN) δ: 149.35 (t, J = 6.3 Hz), 138.02 (app t), 132.75 (s), 131.55 (s), 129.01 (t, J = 2.4 Hz), 128.94 (t, J = 19.2 Hz), 128.74 (t, J = 2.9 Hz), 123.68 (s), 27.92 (t, *J* = 11.6 Hz), 19.41 (t, *J* = 2.8 Hz), 18.37 (s). λ_{max} (THF, nm), ε (M^{-1} cm^{-1}): 307, 9.12 x 10^2; 345, 7.59 x 10^2. Anal. Calcd. for $C_{31}H_{41}F_3NiO_3P_2S$ (%): C, 55.46; H, 6.16. Found: C, 55.04; H, 5.88. MS (m/z): calcd, 521.2037 (M^+[-OTf]); found 521.2011 (FAB-MS, M^+[-OTf]).

NMR of 5·OTf in CD_2Cl_2. **5·OTf** could not be isolated cleanly in CD_2Cl_2 without traces of **6·OTf** or **7·OTf**. ^{1}H NMR (300 MHz, CD_2Cl_2) δ: 7.87 – 7.44 (m, 8H, aryl-*H*), 6.87, (br s, 4H, central aryl-*H*), 2.45 (m, 4H, C*H*$(CH_3)_2$), 1.19 – 0.96 (app m, 24H, CH(C*H*$_3)_2$), -17.57 (t, $J_{P\text{-}H}$ = 67.8 Hz, 1H, Ni-*H*). ^{31}P NMR (121 MHz, CD_3CN) δ: 38.87 (app m).

Thermal conversion of 5·OTf to 6·OTf and 7·OTf. To a stirring suspension of **2** (9.5 mg, 0.017 mmol) in minimal CD_3CN was added TlOTf (6.0 g, 0.017 mmol) with the aid of 0.3 mL CD_3CN. After stirring for 30 min, the reaction was filtered through a plug of glass filter paper into a J. Young NMR tube and diluted to a previously demarcated volume of 0.5 mL with more CD_3CN. The purity of **5·OTf** in solution was verified by room temperature ^{1}H and ^{31}P NMR. A 400 MHz Varian NMR Spectrometer was equilibrated to 75 °C, the sample was inserted into the probe, and locked and shimmed. ^{1}H NMR spectra were collected every 3 minutes. After 1h, the two major species in solution were **5·OTf** and **6·OTf**. After 5h, **5·OTf** and **6·OTf** were mostly consumed, and **7·OTf** was the major species (see Figure S24). At the end of 11h, the sample was ejected, and a dark metallic mirror on the NMR tube wall was evident, suggesting that decomposition may have contributed to the broad unidentified peaks that grew throughout the experiment. Crystallization of **7·OTf** from MeCN/Et_2O yielded light yellow crystals. **7·OTf** Anal. Calcd. for $C_{31}H_{41}F_3NiO_3P_2S$ (%): C, 55.46; H, 6.16. Found: C, 55.12; H, 5.97.

NMR characterization of 6·OTf.

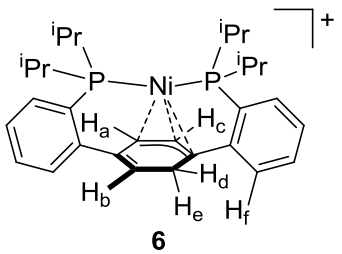

6

Species **6** could not be isolated. Numerous attempts to crystallize mixtures of **5** and **6** resulted in either crystals of **7** or disordered crystals that upon dissolving in CD_3CN, were identified by ^{31}P NMR as a mixture of **5**, **6**, and **7**. Aromatic and isopropyl ^1H NMR peaks of **6** could not be differentiated from those of **5** or **7**, but various correlation experiments were used to assign the protons from the central ring of **6**. 2D gradient COSY revealed the connectivity of the central ring protons (see Figure S16). The shapes of the peaks were more complicated than expected, but simplified upon broadband ^{31}P decoupling using a GARP waveform centered at 55 ppm (see Figure S17), indicating the presence of large $J_{P\text{-}H(central\ ring)}$. To differentiate between H_e (*exo*) and H_d (*endo*) of the sp^3 central ring carbon, 1D NOE experiments were conducted (see Figure S18). Irridation of the peak at 1.78 ppm transferred to an aromatic doublet. This observation was assigned to the NOE between the *exo* proton and the *ortho* proton of the neighboring arene. **6·OTf** ^1H NMR (300 MHz, CD_2Cl_2) δ: 7.56 (1H, H_f), 5.76 (1H, H_a), 5.70 (1H, H_b), 5.18 (1H, H_c), 2.85 (1H, H_d), 1.78 (1H, H_e). ^{31}P NMR (121 MHz, CD_3CN) δ: 61.11 (*d*, J_{PP} = 10.9 Hz), 35.45 (*d*, J_{PP} = 10.9 Hz).

Protonation of 1 and isolation of 7·BAr$_{F24}$.

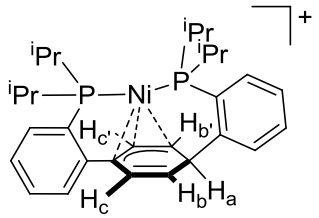

7

To a red solution of **1** (30.4 mg, 0.06 mmol) in THF (2 mL) was added $[H(OEt_2)][B(C_6H_3(CF_3)_2)_4]$ (59.0 mg, 0.06 mmol). ^{31}P NMR at this stage indicates that a mixture of **5·BAr$_{F24}$**, **6·BAr$_{F24}$**, and **7·BAr$_{F24}$** was present. After stirring for 30 minutes at room temperature, volatiles were removed under vacuum. The crude product was washed with hexanes to remove trace unreacted **1**, and then filtered through Celite as a Et_2O solution. The filtrate was concentrated under vacuum to a solid. A DCM solution of this solid was layered under pentane, and dark brown XRD-quality crystals of **7·BAr$_{F24}$** (58.0 mg, 72% yield) were formed at -35 °C over three days. ^1H NMR (400 MHz, CD_3CN) δ: 7.91 (m, 2H, aryl-*H*), 7.69 (br s, 8H, BArF-*H*), 7.67 (br s, 4H, BArF-*H*), 7.56 (m, 4H, aryl-*H*), 7.39 (m, 2H, aryl-*H*), 5.86 (d, J = 8.1 Hz, 2H, H_c and $H_{C'}$, $^1J_{CH}$ = 175.6 Hz), 5.12 (m, 2H, H_b and $H_{b'}$, $^1J_{CH}$ = 167.6 Hz), 2.59 (m, 5H, C*H*$(CH_3)_2$ and H_a), 1.10 (m, 24H, CH(C*H*$_3)_2$). ^{31}P NMR (121 MHz, CD_3CN) δ: 58.80 (*d*, J_{PP} = 1.6 Hz), 50.44 (*d*, J_{PP} = 1.6 Hz). ^{13}C NMR (101 MHz, CD_2Cl_2, not all carbons were observed) δ: 163.06 (s), 162.57 (s), 162.07 (s), 161.58 (s), 135.289 (d, J = 19.1 Hz), 133.15 (m), 132.57 (m), 131.20 (app d), 129.30 (app q), 127.87 (br s), 126.53 (s), 118.16 (d, J = 22.5 Hz), 97.32 (br m), 97.105 (app d), 30.31 (s), 27.32 (m), 25.94 (m), 20.23 (m), 19.52 (m), 18.89 (m), 18.57 (m). The chemical shift of H_a was determined to overlap with the methine protons by integration of ^1H NMR data (see Figure S20) and by a COSY experiment that showed correlation with H_b (see Figure S21).

Thermal conversion of 5-*d*$_4$·OTf to partially deuterated 6·OTf. To a suspension of **2-*d*$_4$** (7.2 mg, 0.0128 mmol) in CD_3CN (0.4 mL) was added TlOTf (4.5 mg, 0.0128 mmol). The solution was allowed to stir for 30 min and then filtered thru a plug of Celite into a J. Young NMR tube. The vial and filter were washed with CD_3CN into the NMR tube until a predemarcated total volume of 0.5 mL was reached. The NMR tube was sealed and placed in a 75 °C oil bath. The reaction was monitored by NMR over 24h, after which it was determined that sufficient conversion had occurred. Due to the formation of a partial mirror on the NMR tube walls, the reaction mixture was filtered through Celite, volatiles were removed, and the crude was redissolved in CD_2Cl_2 in a clean NMR tube, which allows for better resolution of the aliphatic ^1H NMR peaks. A major doublet was observed at 2.85 ppm (*endo* proton of **6**), and a minor multiplet was present at ~1.78 ppm. Assuming that the multiplet at 1.78 corresponded to the exo proton and not an impurity, the ratio of *endo*:*exo* 1H incorporation is 90:10 (see Figure S26).

Chloride addition to a mixture of 5·OTf, 6·OTf, and 7·OTf. A solution of **5·OTf** (9.4 mg, 0.0140 mmol) in THF (0.5 mL) was loaded in a J. Young NMR tube and placed in a 70 °C oil bath. After 1h, the NMR tube was washed with hexanes to remove oil and allowed to cool to room temperature. ^{31}P NMR indicated a mixture of **5·OTf**, **6·OTf**, and **7·OTf**

in solution. Volatiles were removed under vacuum, and the resulting solids were redissolved in CD_2Cl_2. An initial ^1H NMR spectrum was collected. Then NBu_4Cl (4.3 mg, 0.0154 mmol) was added to the mixture and an intermediate spectrum was recorded. Finally, another portion of NBu_4Cl (11.7 mg, 0.042 mmol) was added and a final spectrum was recorded. Integration of ^1H NMR peaks at 6.82 and -28.90 ppm and regions 5.90-5.60 and 5.26-5.05 ppm were used to determine to relative concentrations of **2**, **5·OTf**, **6·OTf**, and **7·OTf** throughout the reaction. It was determined that a 62:26:12 mixture of **6·OTf**, **5·OTf**, and **7·OTf** was transformed into a 85:15 mixture of **2** and **7·OTf** (see Figure S25).

1,8-Diazabicyclo[5.4.0]undec-7-ene addition to a mixture of 5·OTf, 6·OTf, and 7·OTf. A solution of **5·OTf** (7.0 mg, 0.0104 mmol) in THF (0.5 mL) was loaded in a J. Young NMR tube and placed in a 70 °C oil bath. After 1h, the NMR tube was washed with hexanes to remove oil and allowed to cool to room temperature. ^{31}P NMR indicated a mixture of **5·OTf**, **6·OTf**, and **7·OTf** in solution. Volatiles were removed under vacuum, and the resulting solids were redissolved in CD_3CN. Initial ^1H and ^{31}P NMR spectra were collected. Then 1,8-diazabicyclo[5.4.0]undec-7-ene (DBU, 2.34 μL, 0.0155 mmol) was added to the mixture, and an intermediate spectrum was recorded, indicating full consumption of **6·OTf** and **7·OTf**. **5·OTf** persisted, however, even 30 min after addition of more DBU (10.0 μL, 0.0662 mmol). However after 12h, colorless crystals were formed the NMR tube, and NMR of the solution indicated full conversion of **6·OTf** to **1**.

Determination of equilibrium dissociation constant of MeCN to 5·OTf. A solution of **5·OTf** (7.6 mg, 0.0113 mmol) in CD_2Cl_2 (0.4 mL) was loaded in a septum-capped NMR tube. A starting ^1H NMR spectrum was collected, and then a microsyringe was used to inject increments of 1:1 MeCN/CD_2Cl_2 or neat MeCN. The chemical shift of the hydride peak shifted upon addition of more MeCN. Assuming that δ(Ni-*H*) in neat CD_3CN corresponds to **5-NCMe**, a normalized measure of the relative concentrations of [**5-NCMe**] and [**5**] is definable as $\Delta\delta = [\delta(\text{Ni-}H) - \delta(\text{Ni-}H)_{CD2Cl2}]/[\delta(\text{Ni-}H)_{CD3CN} - \delta(\text{Ni-}H)_{CD2Cl2}] = [\textbf{5-NCMe}]/[\textbf{5}]_{total}$. Because $K_d = [\textbf{5}][MeCN]/[\textbf{5-NCMe}]$, then $\Delta\delta = [MeCN]/([MeCN] + K_d)$, and fitting $1/\Delta\delta$ vs 1/[MeCN] yields K_d = 1.13 M (see Figure S27).

Deprotonation of hydride complexes with dimethylbenzylamine. A stock solution of **2** (21.8 mg, 0.0391 mmol) in THF (1.6 mL) was prepared. 0.5 mL of this orange solution (0.0122 mmol **2**) was transferred into an NMR tube. A coaxial insert was loaded with a saturated THF solution of 1,2-bisdiphenylphosphinoethane (dppe) and placed in the same NMR tube. A preliminary ^{31}P NMR spectrum was collected. One equivalent of dimethylbenzylamine (DMBA, 1.8 μL, 0.0122 mmol) was added to the NMR tube, causing the emergence of a deep red color upon mixing. Another ^{31}P NMR spectrum was taken and indicated the generation of **1**. The relative integrations of the signals for **2** and dppe were used to calculate 22% deprotonation of **2**. An identical procedure was used to determine 26% deprotonation of **5·OTf** by 1 equivalent of DMBA (see Figure S28).

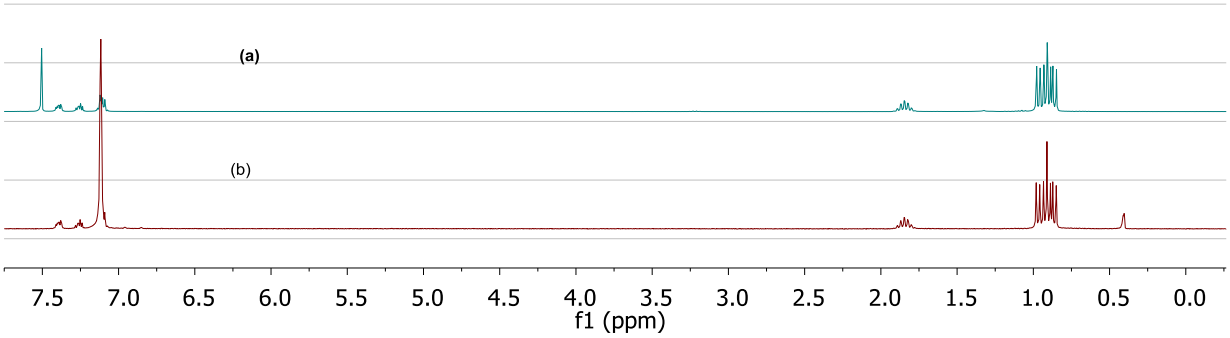

Figure S1. ^{1}H NMR spectra of (a) **4** and (b) **4-*d*$_4$** (C_6D_6, 300 MHz)

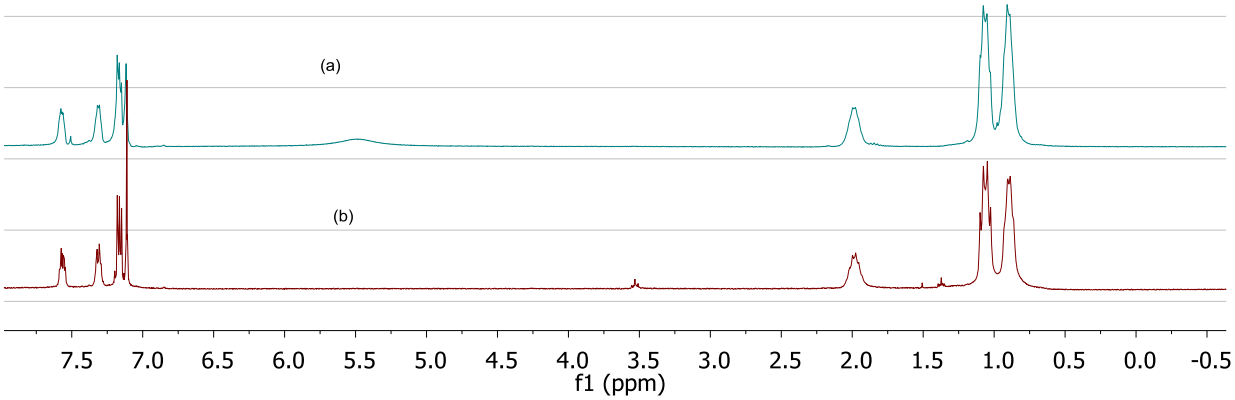

Figure S2. ^{1}H NMR spectra of (a) **1** and (b) **1-*d*$_4$** (C_6D_6, 300 MHz)

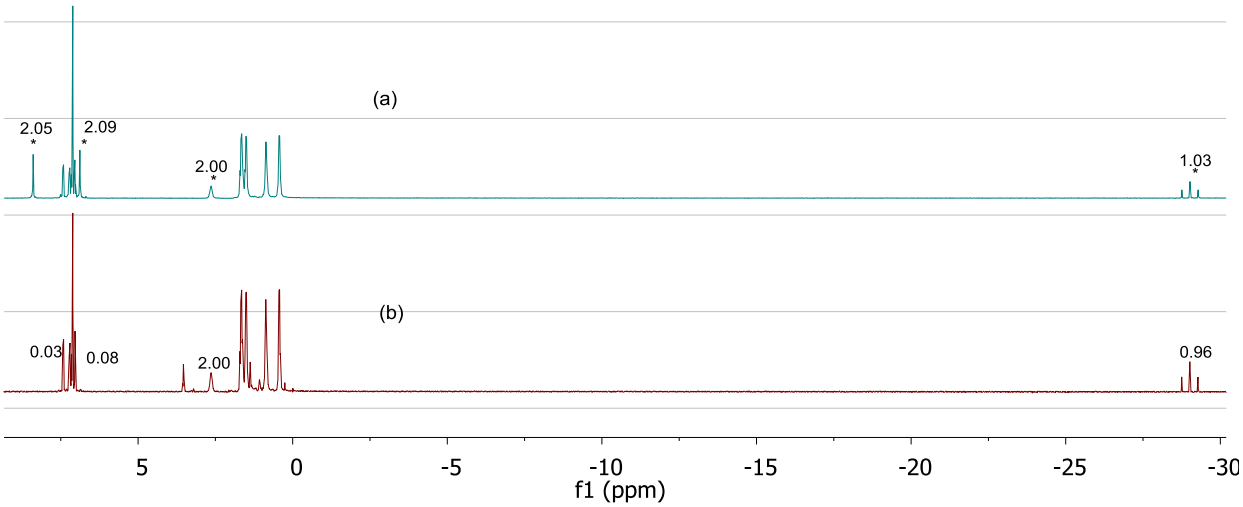

Figure S3. ^{1}H NMR spectra of (a) **2** and (b) **2-*d*$_4$** (C_6D_6, 300 MHz)

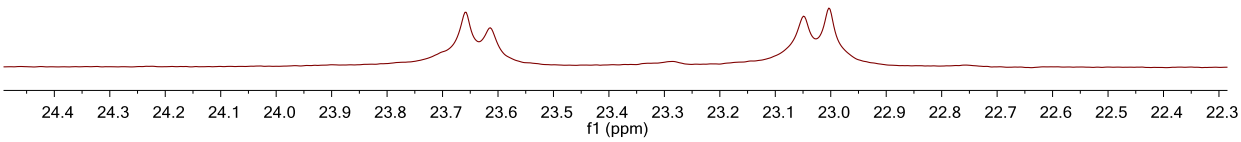

Figure S4. $^{31}P\{^{1}H\}$ NMR spectrum of **2** (C_6D_6, 300 MHz)

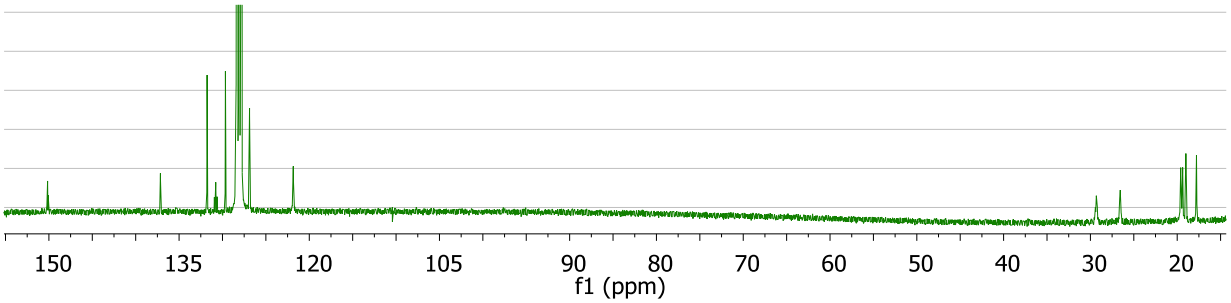

Figure S5. $^{13}C\{^{1}H\}$ NMR spectrum of **2** (C_6D_6, 400 MHz)

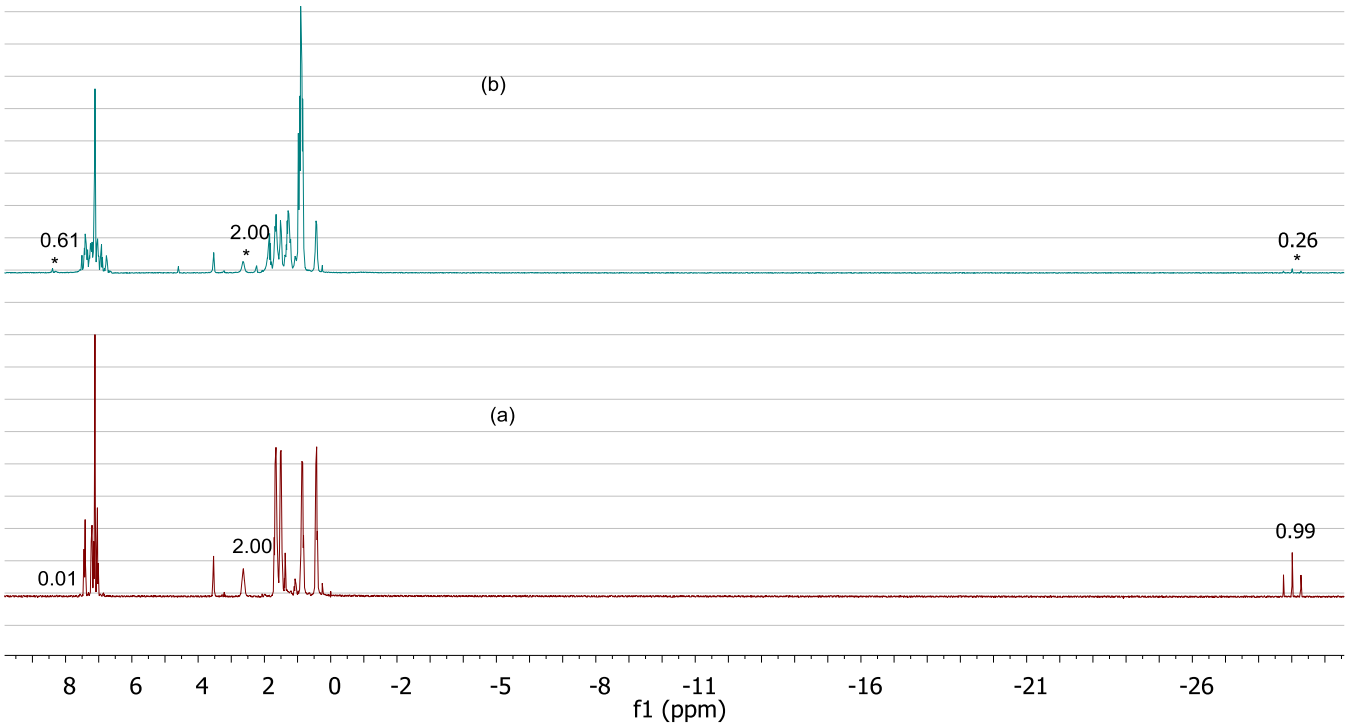

Figure S6. ^{1}H NMR spectra (C_6D_6, 300 MHz) monitoring isotopic scrambling of **2-*d*$_4$** with concomitant conversion to partially deuterated **3** and **4**. (a) starting **2-*d*$_4$** (b) the same sample after 12 h in a 70 °C oil bath (~48% conversion relative to internal THF standard)

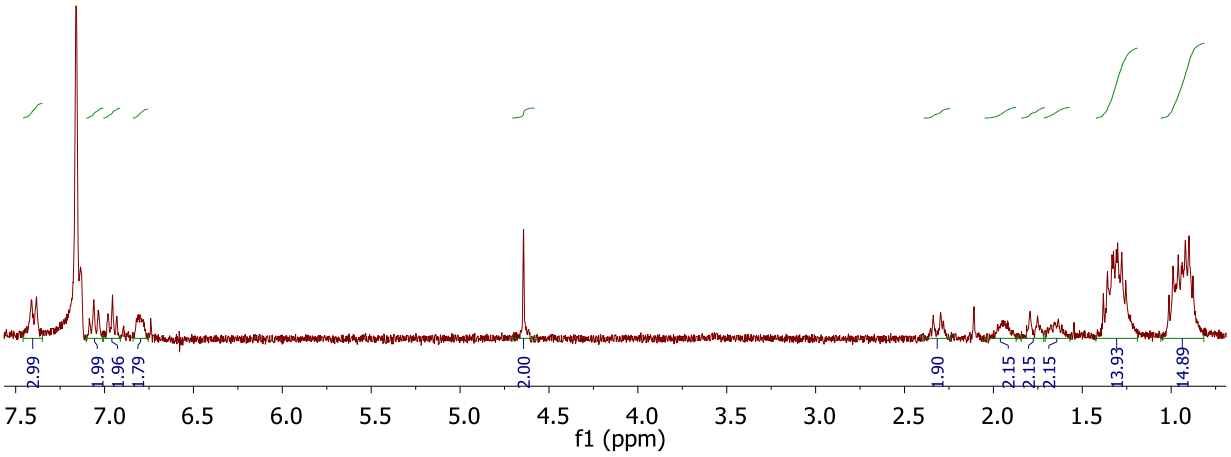

Figure S7. ^{1}H NMR spectrum of **3** (C_6D_6, 600 MHz)

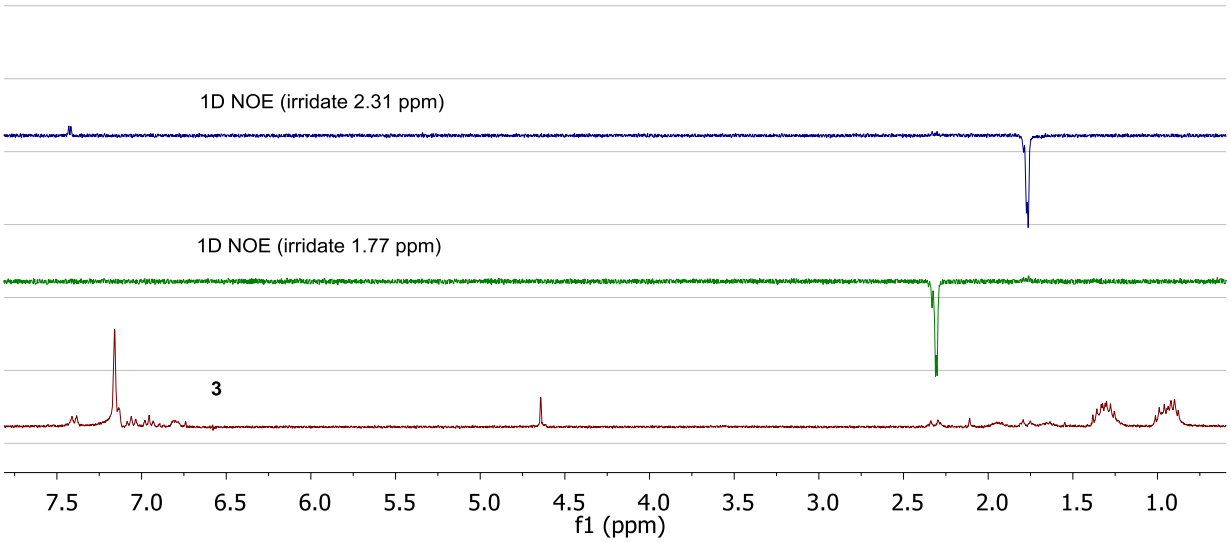

Figure S8. 1D ^{1}H NOE experiments of **3** (C_6D_6, 600 MHz)

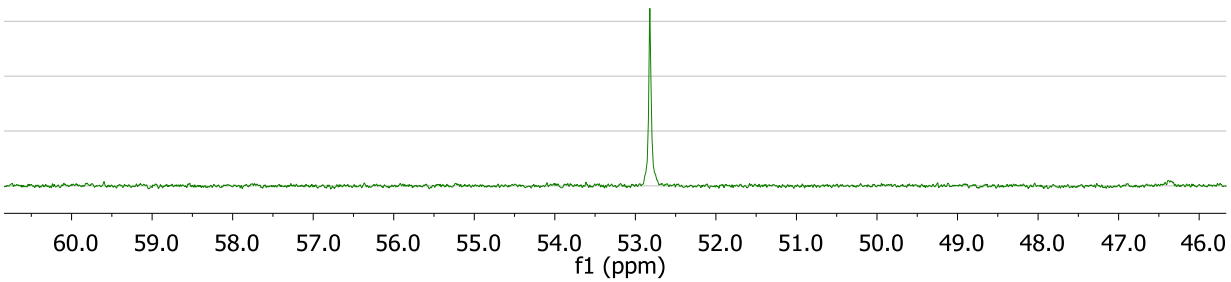

Figure S9. ^{31}P{^{1}H} NMR spectrum of **3** (C_6D_6, 121 MHz)

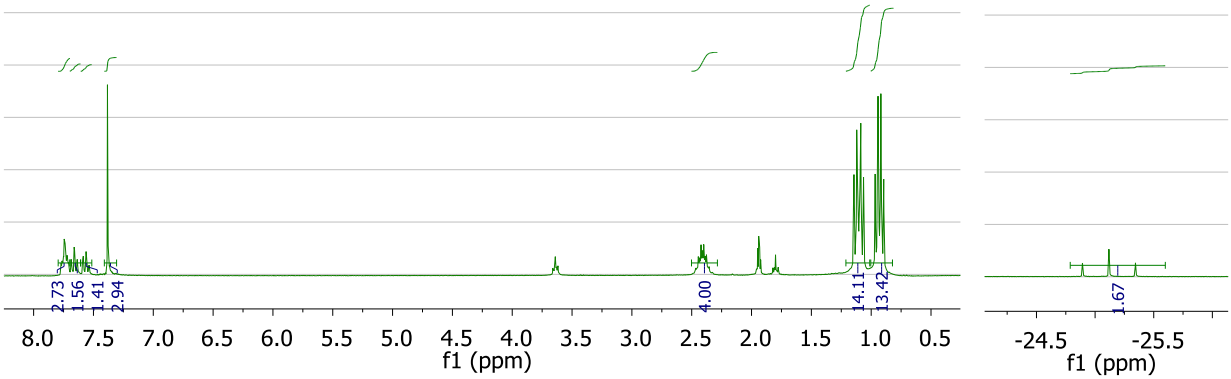

Figure S11. ^{1}H NMR spectra of **5·OTf** in CD_3CN (400 MHz)

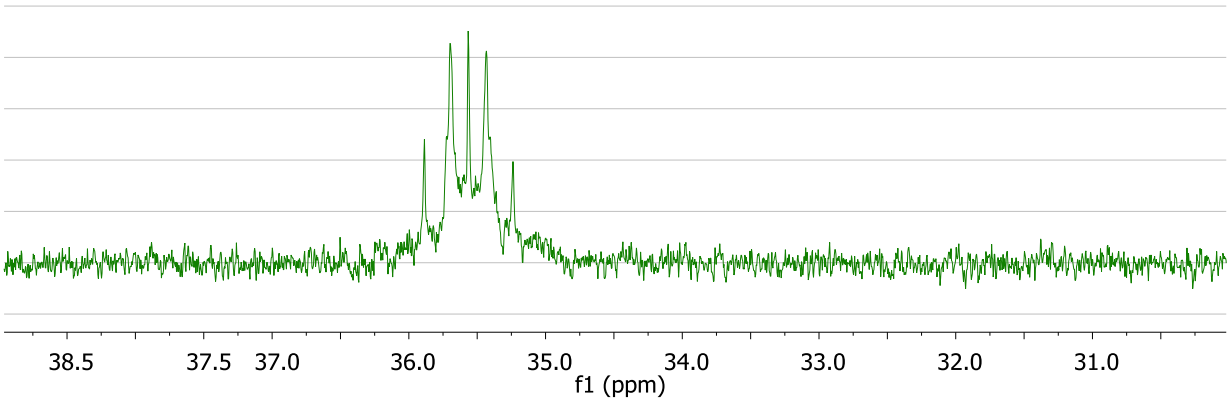

Figure S12. ^{31}P NMR spectra of **5·OTf** in CD_3CN (161 MHz)

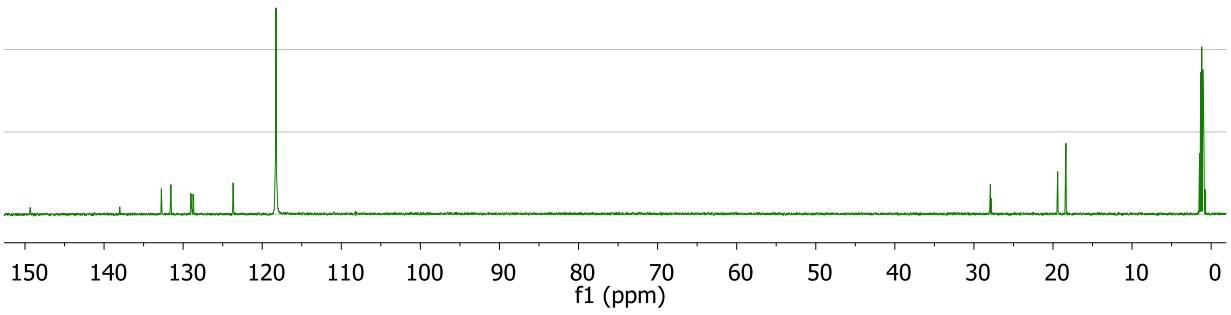

Figure S13. $^{13}C\{^{1}H\}$ NMR spectrum of **5·OTf** (CD_3CN, 101 MHz)

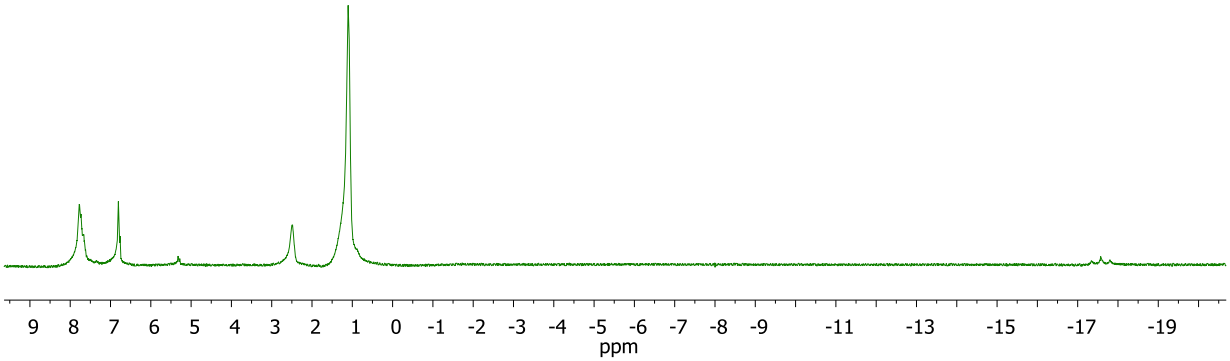

Figure S14. ^{1}H NMR spectra of **5·OTf** (>95%) in CD_2Cl_2 (300 MHz)

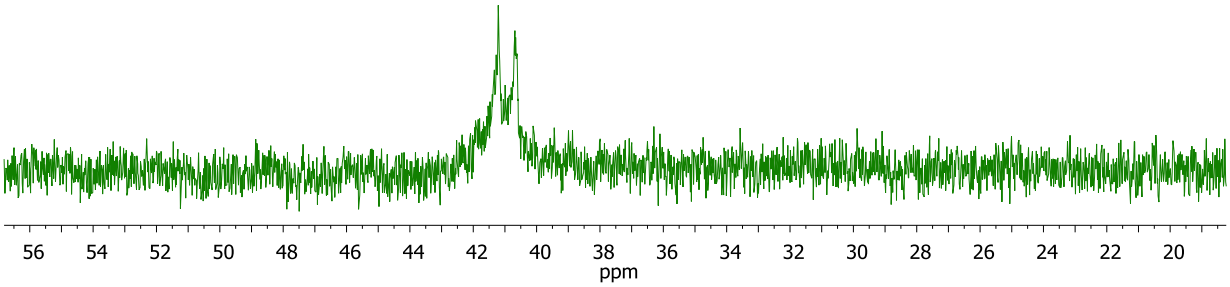

Figure S15. ^{31}P{^{1}H} NMR spectra of **5·OTf** (>95%) in CD_2Cl_2 (161 MHz)

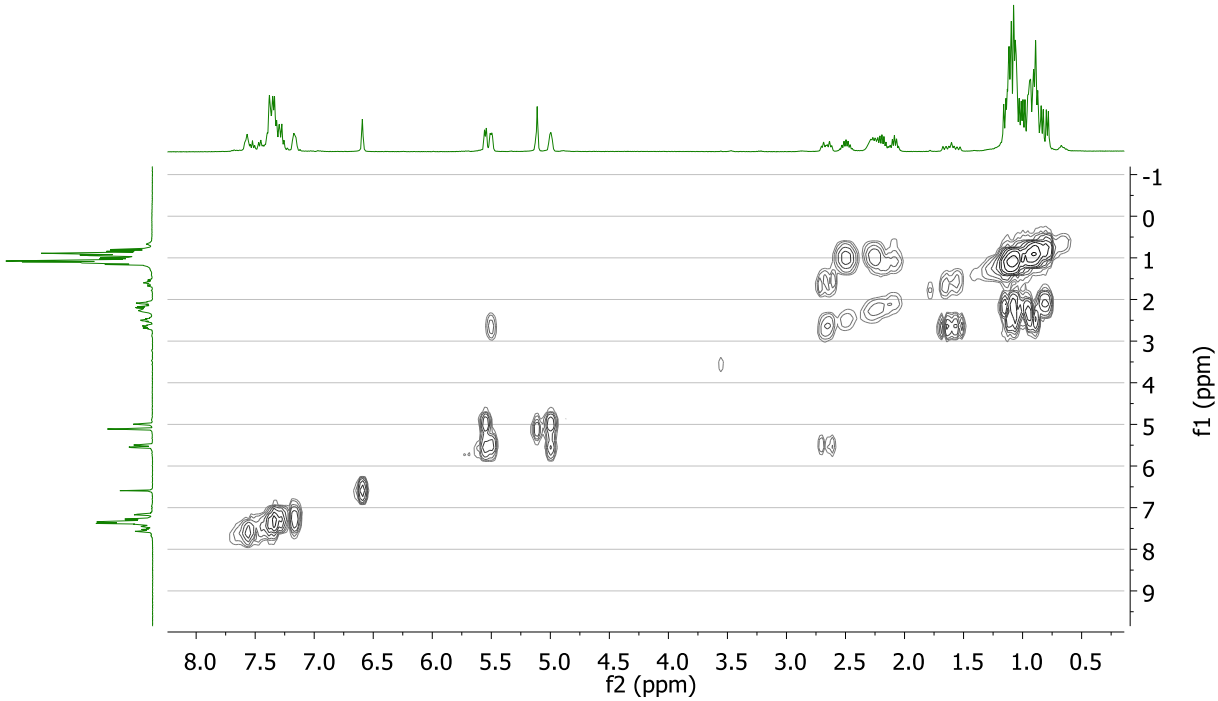

Figure S16. Gradient COSY spectrum of a mixture of **5·OTf** and **6·OTf** (CD_2Cl_2, 400 MHz)

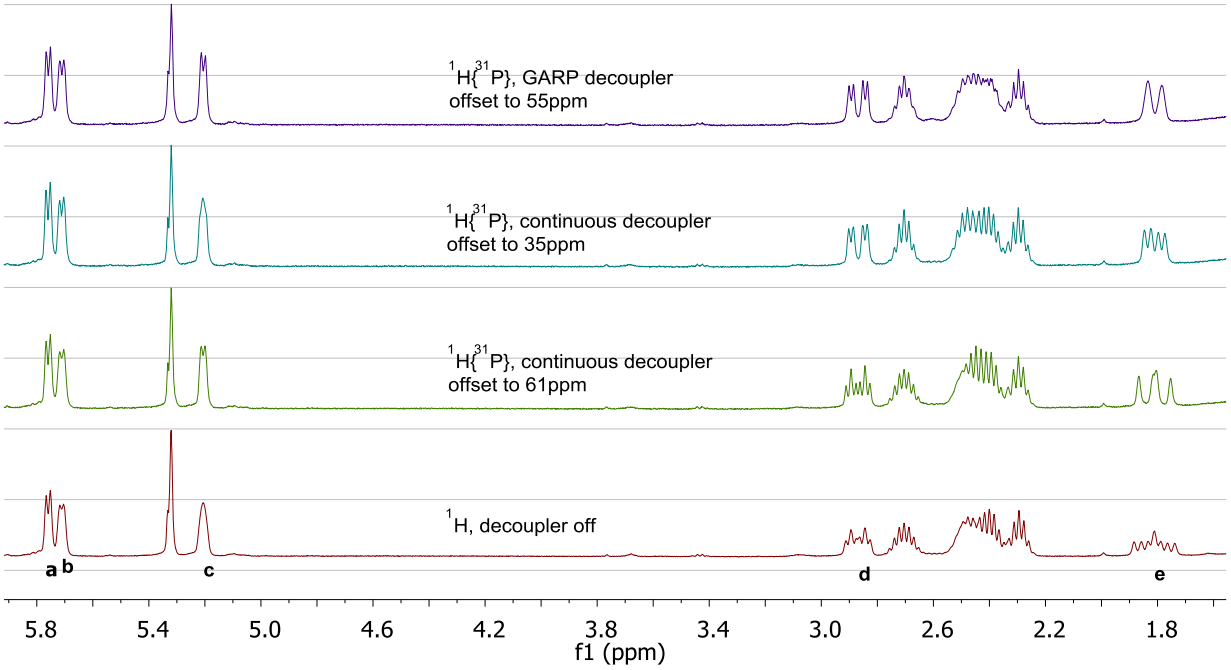

Figure S17. ^1H NMR spectra of a mixture of **5·OTf** and **6·OTf** with various ^{31}P decoupling methods (CD_2Cl_2, 400 MHz)

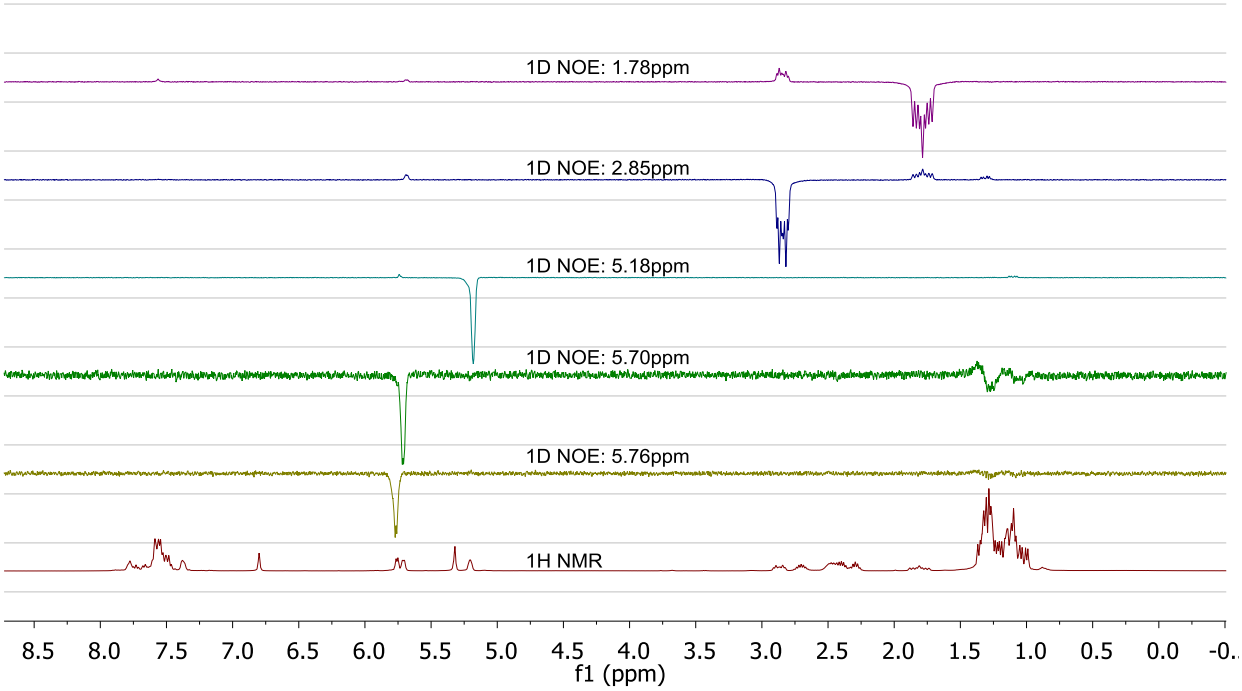

Figure S18. ^1H NMR and 1D NOE spectra of a mixture of **5·OTf** and **6·OTf** (CD_2Cl_2, 400 MHz)

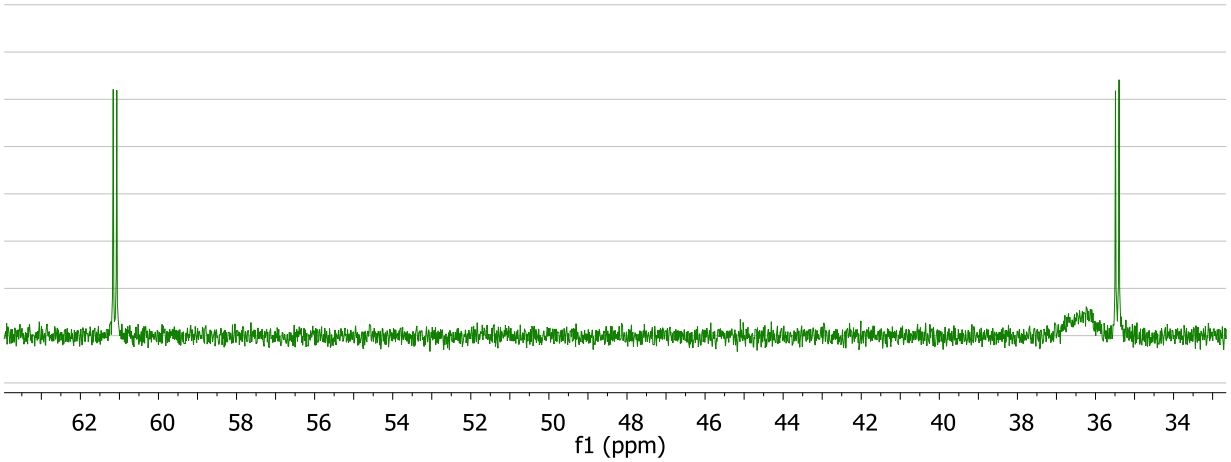

Figure S19. $^{31}P\{^{1}H\}$ NMR spectrum of a mixture of **5·OTf** and **6·OTf** (CD_2Cl_2, trace CD_3CN, 161 MHz)

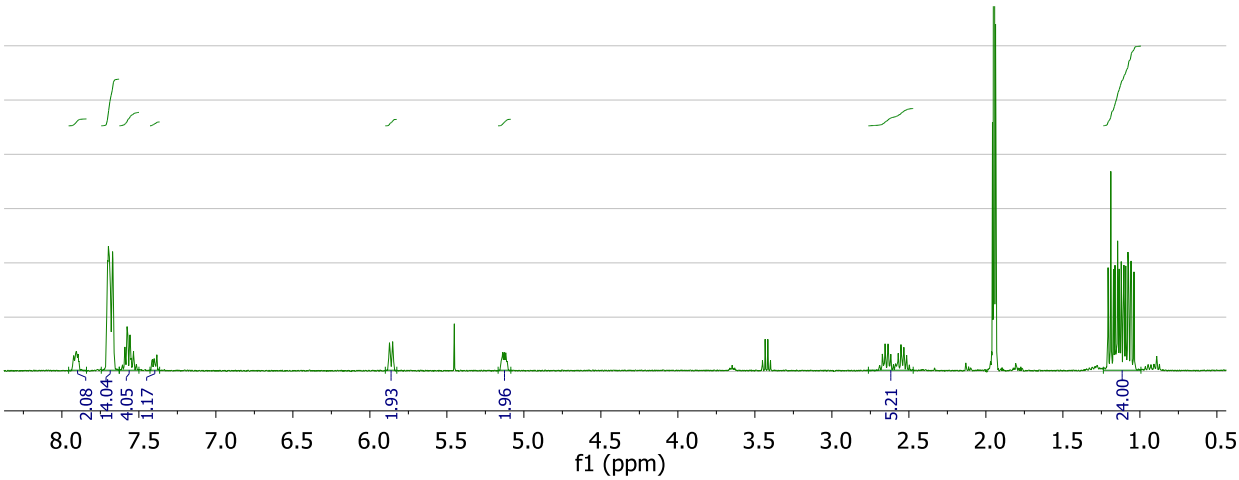

Figure S20. ^{1}H NMR spectrum of **7·BAr$_{F24}$** (CD_3CN, 600 MHz)

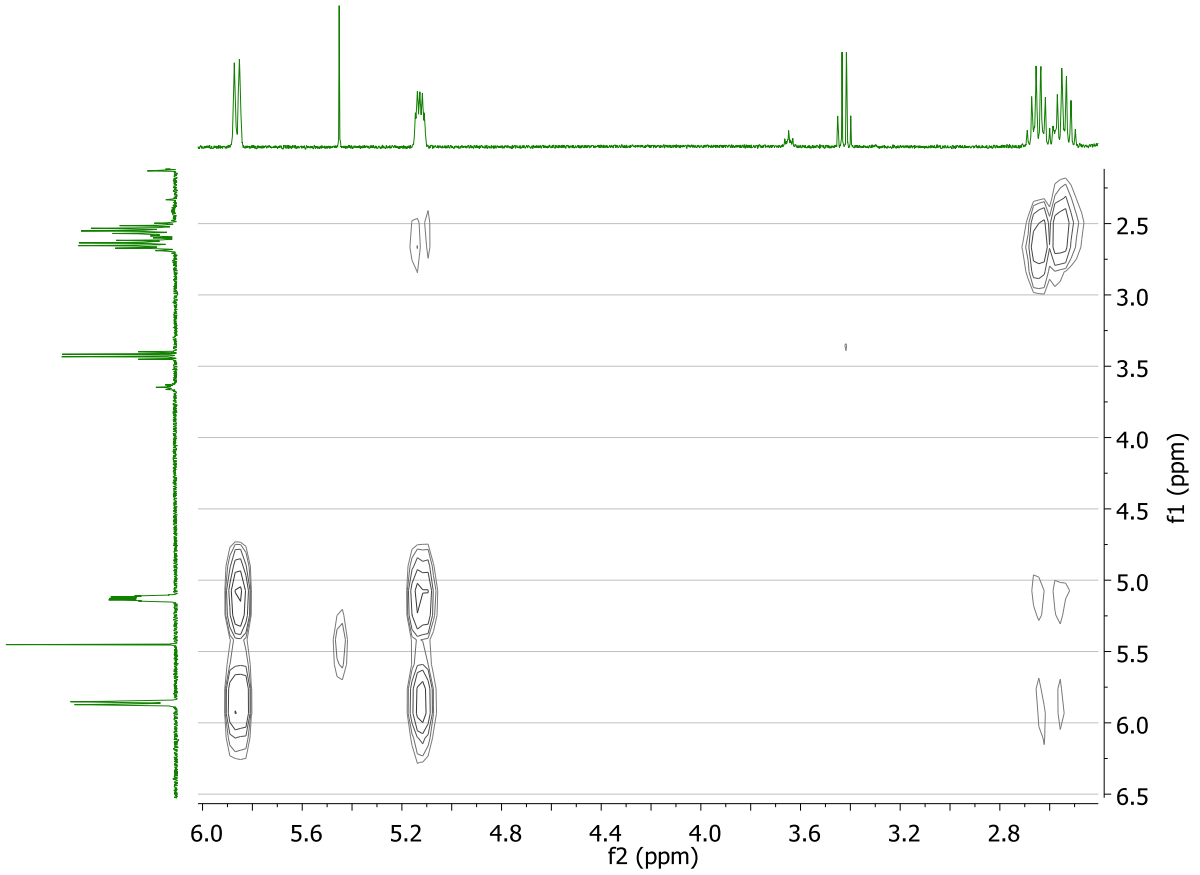

Figure S21. Gradient COSY spectrum of **7·BArF$_{24}$** (CD_3CN, 600 MHz)

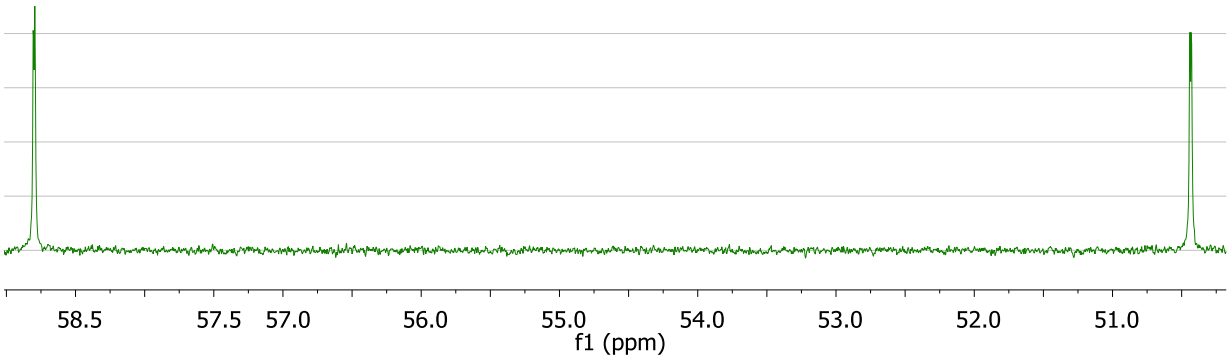

Figure S22. $^{31}P\{^{1}H\}$ NMR spectrum of **7·BArF$_{24}$** (CD_3CN, 162 MHz)

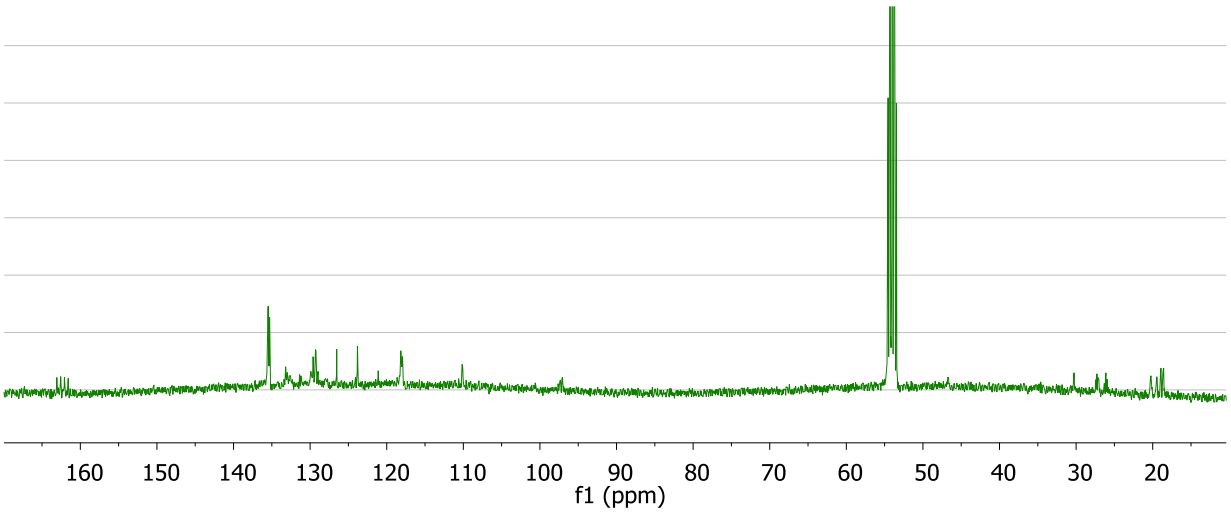

Figure S23. $^{13}C\{^{1}H\}$ NMR spectrum of **7·BArF$_{24}$** (CD_2Cl_2, 101 MHz)

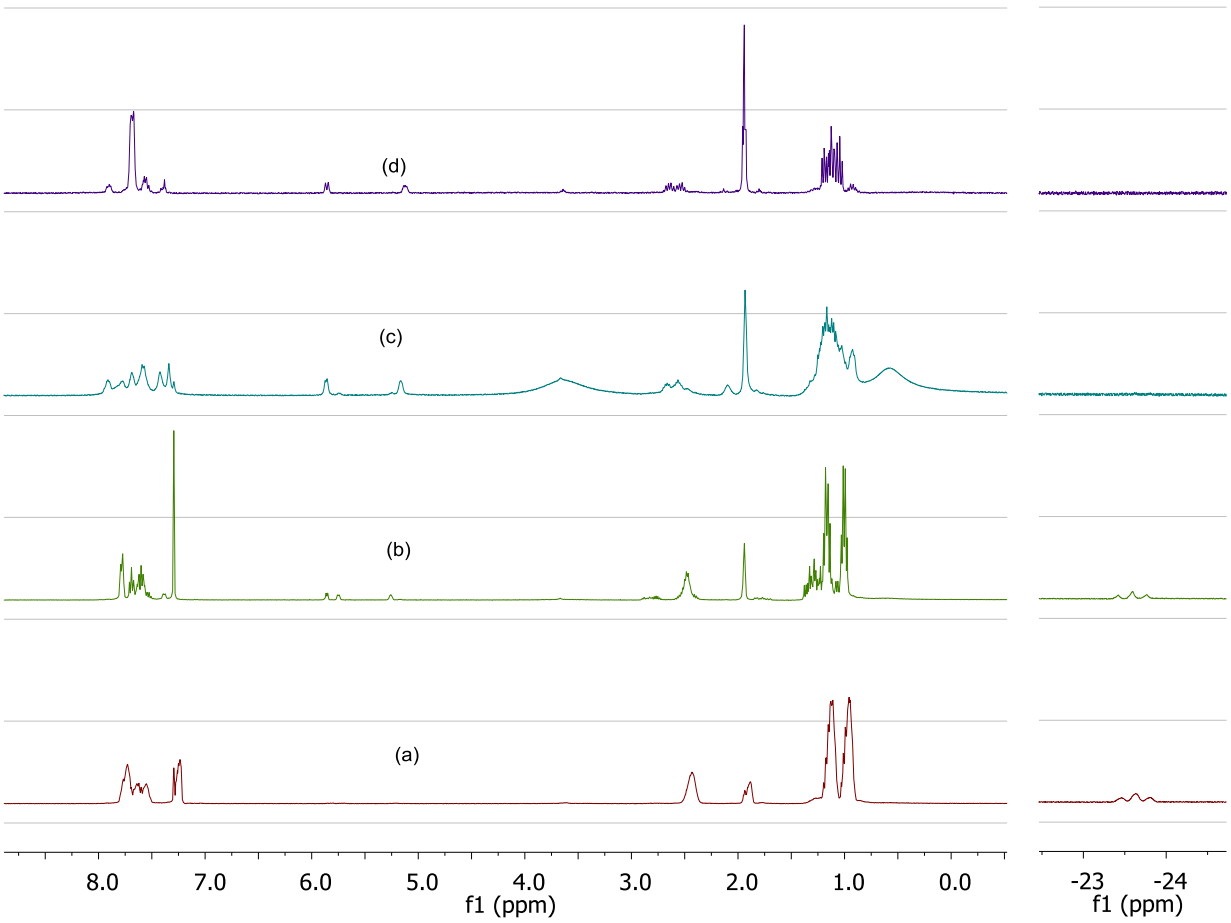

Figure S24. ^{1}H NMR spectra (CD_3CN, 400MHz, 75 °C) monitoring sequential thermal conversion of **5·OTf** to **6·OTf** to **7·OTf**. (a) 3 min (b) 57 min (c) 303 min (d) **7·BAr$_{F24}$** for comparison.

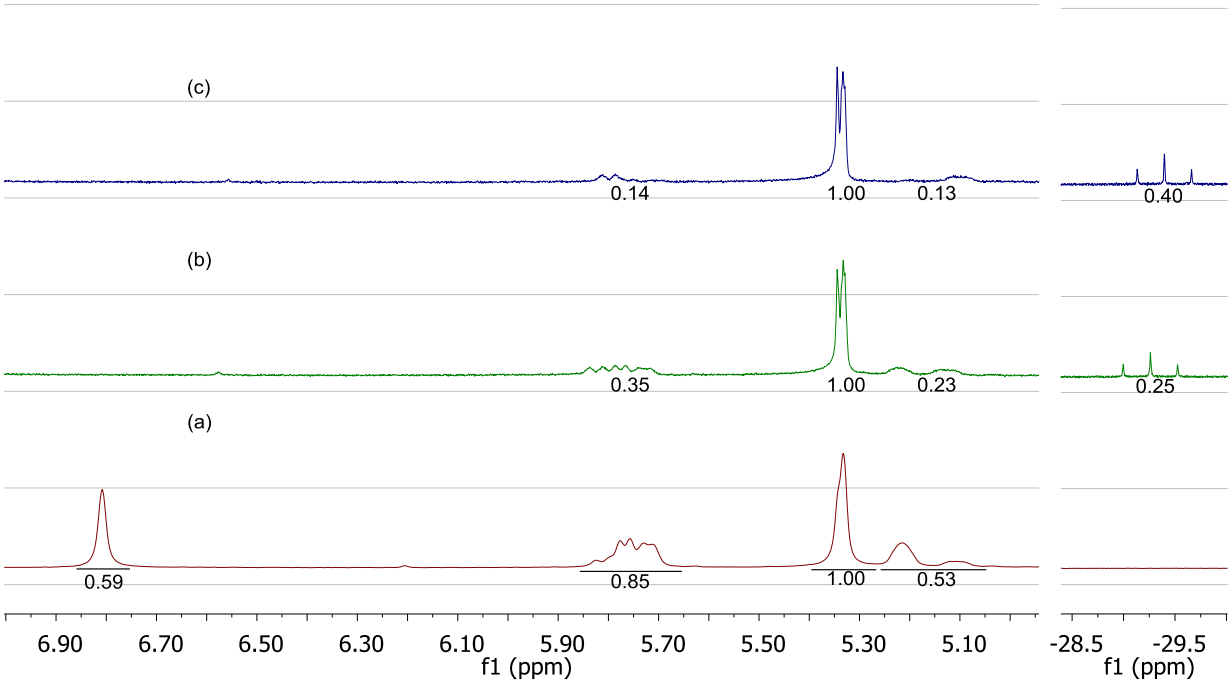

Figure S25. ^{1}H NMR spectra (CD_2Cl_2, 300 MHz) monitoring the effect of chloride addition to a mixture of **5·OTf**, **6·OTf**, and **7·OTf**. (a) Initial mixture before NBu_4Cl addition (b) Intermediate mixture after addition of 1.1 equiv. NBu_4Cl (c) Final mixture after addition of 3 more equiv. NBu_4Cl.

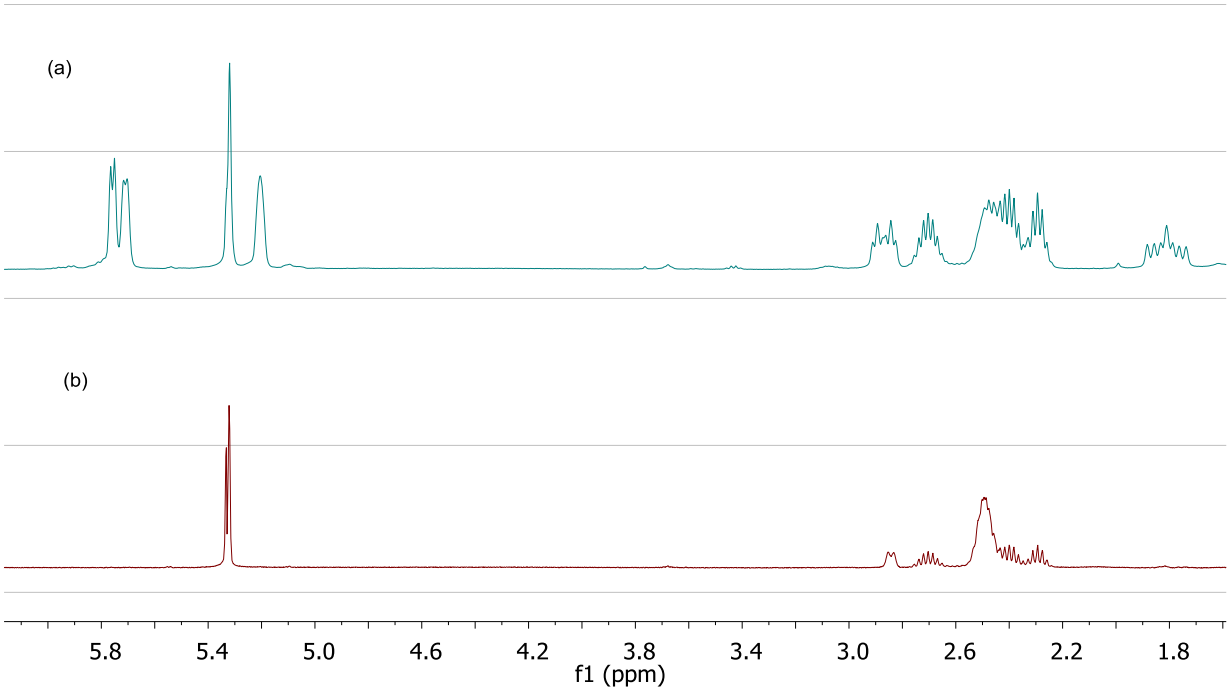

Figure S26. ^{1}H NMR spectra (CD_2Cl_2, 400 MHz) of mixtures of **5·OTf** and **6·OTf** generated from (a) **5·OTf** and (b) **5-*d*$_4$·OTf**.

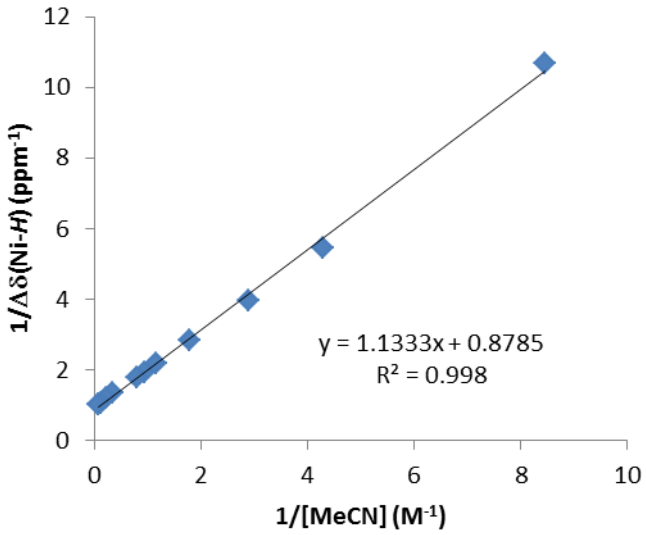

Figure S27. Titration of MeCN into CD_2Cl_2 solution of **5·OTf**.

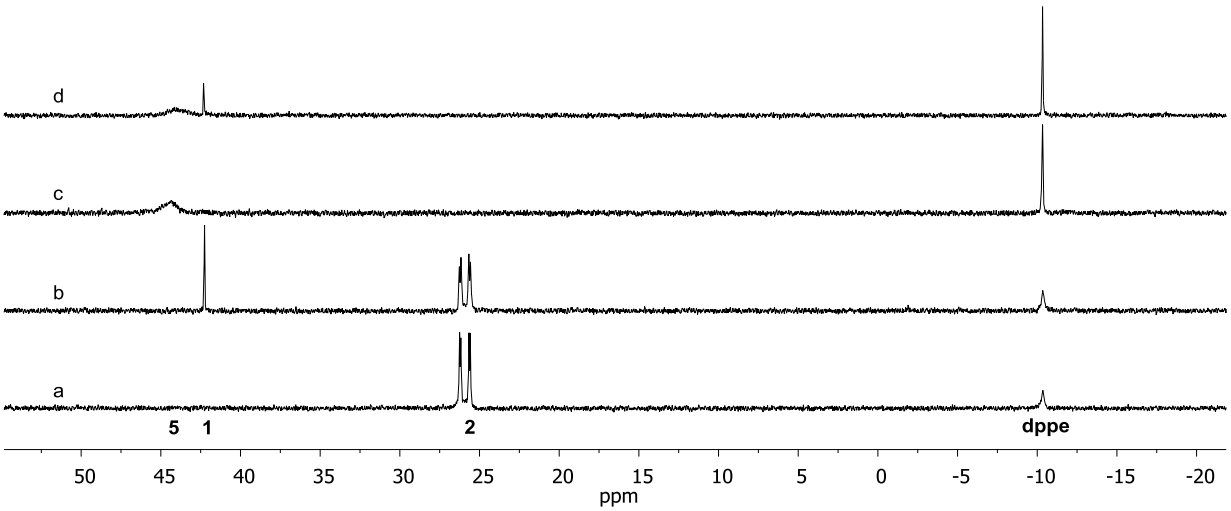

Figure S28. ^{31}P NMR spectra monitoring deprotonation of hydride complexes by dimethylbenzylamine (DMBA), relative to 1,2-bisdiphenylphosphinoethane: (a) 2 (b) 2 + 1 equiv. DMBA (c) 5 (d) 5 + 1 equiv. DMBA.

Crystallographic Information

General Considerations. Crystallographic data have been deposited at the CCDC, 12 Union Road, Cambridge CB2 1EZ, UK and copies can be obtained on request, free of charge, by quoting the publication citation and the deposition numbers listed in Table S#.

Table S1. Crystal and refinement data for **2**, **3**, **5·OTf + 5-NCMe·OTf**, and **7·BAr$_{F24}$**,

	2	**3**	**5·OTf + 5-NCMe·OTf**	**7·BAr$_{F24}$**
CCDC Deposition #	782511	800343	800346	800345
Empirical formula	$C_{30}H_{41}ClP_2Ni$	$C_{30}H_{42}P_2Cl_2Ni_2$	$[C_{30}H_{40}P_2NiH]+$ $[C_{32}H_{43}NP_2NiH]$ + $2[CF_3O_3S]^-$	$[C_{30}H_{41}P_2Ni]+$ $[C_{32}H_{12}BF_{24}]^-$
Formula weight	557.73	652.9	691.88	1385.5
Crystallization Solvent	Toluene/pentane	Pentane/toluene	Acetonitrile/diethyl ether	THF/pentane
Crystal Habit	Block	Fragment	Block	Block
Crystal size, mm^3	0.17 x 0.13 x 0.11	0.21 x 0.15 x 0.11	0.24 x 0.22 x 0.21	0.27 x 0.22 x 0.13
Crystal color	Orange	Dark purple	Yellow	Red
θ range for lattice determination	2.29 to 26.38°	2.29 to 35.93°	2.24 to 29.58°	2.24 to 24.50°
a, Å	8.6569(3)	10.9521(4)	27.7671(12)	18.8883(8)
b, Å	23.2021(8)	16.7037(7)	12.6722(6)	18.2168(8)
c, Å	14.5399(5)	17.0594(7)	20.3587(9)	19.5092(8)
α, °	90	90	90	90
β, °	106.911(2)	106.816(2)	112.212(2)	116.405(2)
γ, °	90	90	90	90
Volume, Å^3	2794.17(17)	2987.4(2)	6632.0(5)	6012.5(4)
Z	4	4	8	4
Crystal system	Monoclinic	Monoclinic	Monoclinic	Monoclinic
Space group	P $2_1/n$	P $2_1/n$	P $2_1/c$	P $2_1/c$
Density (calculated)	1.326 Mg/m^3	1.452 Mg/m^3	1.386 Mg/m^3	1.531 Mg/m^3
F(000)	1184	1368	2904	2816
θ range for data collection, °	1.71 to 26.43	1.74 to 36.01	1.79 to 30.57	2.09 to 30.56
Completeness to θ = 26.43°	99.9%	99.4%	99.4%	94.0%
Index ranges	$-10 \le h \le 9$ $-29 \le k \le 29$ $-18 \le l \le 18$	$-18 \le h \le 18$ $-27 \le k \le 26$ $-28 \le l \le 28$	$-39 \le h \le 39$ $-17 \le k \le 17$ $-29 \le l \le 29$	$-25 \le h \le 26$ $-25 \le k \le 25$ $-27 \le l \le 27$
Data collection scan type	ω scans; 10 settings	ω scans; 11 settings	ω scans; 9 settings	ω scans; 11 settings
Reflections collected	47613	112796	156014	162138
Independent reflections	5744 [R_{int}= 0.0538]	14075 [R_{int}= 0.0504]	20232 [R_{int}= 0.0733]	17311 [R_{int}= 0.0697]
Absorption coefficient, mm^{-1}	0.922	1.565	0.794	0.491

Absorption correction	Gaussian	None	None	None
Max. and min. transmission	0.9150 and 0.8629	0.8467 and 0.7347	0.8511 and 0.8324	0.9389 and 0.8789
Hydrogen placement	Geometric positions	Difference Fourier map	Difference Fourier map	Geometric positions
Structure refinement program	SHELXL-97 (Sheldrick, 2008)	SHELXL-97 (Sheldrick, 2008)	SHELXL-97 (Sheldrick, 2008)	SHELXL-97 (Sheldrick, 2008)
Refinement method	Full matrix least-squares on F2	Full matrix least-squares on F2	Full matrix least-squares on F2	Full matrix least-squares on F2
Data / restraints / parameters	5744 / 0 / 471	14075 / 0 / 493	20232 / 0 / 1143	17311 / 0 / 917
Treatment of hydrogen atoms	Riding	Unrestrained	Unrestrained	Riding
Goodness-of-fit on F2	1.759	1.552	2.908	1.7
Final R indices [I>2σ(I), 4802 reflections]	R1 = 0.0302 *w*R2 = 0.0476	R1 = 0.0268 *w*R2 = 0.0426	R1 = 0.1001 *w*R2 = 0.0925	R1 = 0.0479 *w*R2 = 0.0568
R indices (all data)	R1 = 0.0397 *w*R2 = 0.0482	R1 = 0.0395 *w*R2 = 0.0432	R1 = 0.1199 *w*R2 = 0.0934	R1 = 0.0911 *w*R2 = 0.0586
Type of weighting scheme used	Sigma	Sigma	Sigma	Sigma
Weighting scheme used	$w=1/\sigma^2(Fo^2)$	$w=1/\sigma^2(Fo^2)$	$w=1/\sigma^2(Fo^2)$	$w=1/\sigma^2(Fo^2)$
Max shift/error	0.001	0.003	0.001	0.001
Average shift/error	0	0	0	0
Largest diff. peak and hole, e.Å^{-3}	0.537 and -0.396	0.805 and -0.774	1.634 and -1.287	1.347 and -0.734
Type of diffractometer	Bruker KAPPA APEX II	Bruker KAPPA APEX II	Bruker KAPPA APEX II	Bruker KAPPA APEX II
Wavelength, Å MoKa	0.71073	0.71073	0.71073	0.71073
Data Collection Temperature	100(2) K	100(2) K	100(2) K	100(2) K
Structure solution program	SHELXS-97 (Sheldrick, 2008)	SHELXS-97 (Sheldrick, 2008)	SHELXS-97 (Sheldrick, 2008)	SHELXS-97 (Sheldrick, 2008)
Primary solution method	Direct methods	Direct methods	Direct methods	Direct methods
Secondary solution method	Difference Fourier map	Difference Fourier map	Difference Fourier map	Difference Fourier map

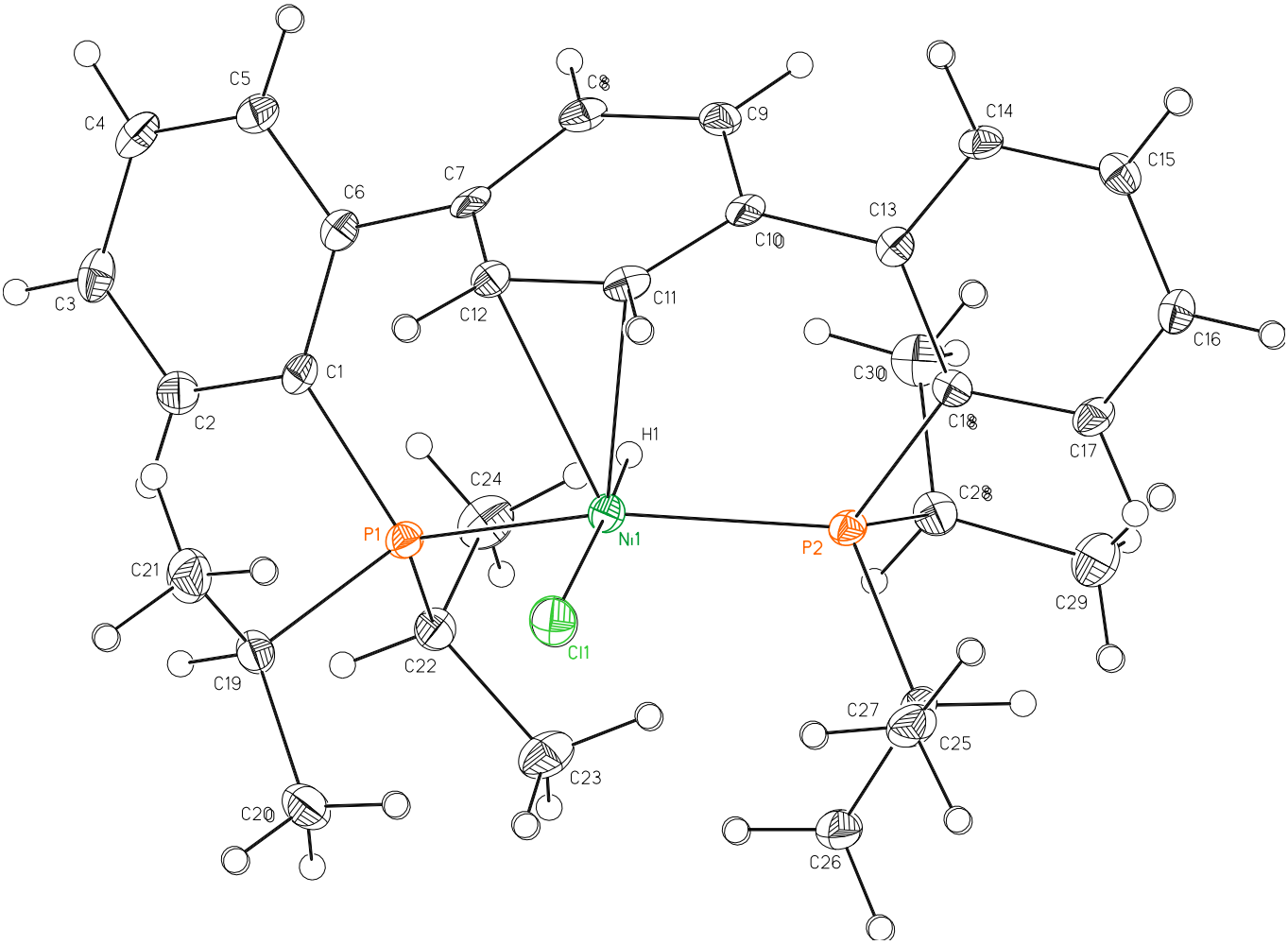

Figure S29. Structural drawing of **2** with 50% thermal probability ellipsoids**.**

Special refinement details for 2. Crystals were mounted on a glass fiber using Paratone oil then placed on the diffractometer under a nitrogen stream at 100K. Refinement of F^2 against ALL reflections. The weighted R-factor (*w*R) and goodness of fit (S) are based on F^2, conventional R-factors (R) are based on F, with F set to zero for negative F^2. The threshold expression of $F^2 > 2\sigma(F^2)$ is used only for calculating R-factors(gt) etc. and is not relevant to the choice of reflections for refinement. R-factors based on F^2 are statistically about twice as large as those based on F, and R-factors based on ALL data will be even larger. All esds (except the esd in the dihedral angle between two l.s. planes) are estimated using the full covariance matrix. The cell esds are taken into account individually in the estimation of esds in distances, angles and torsion angles; correlations between esds in cell parameters are only used when they are defined by crystal symmetry. An approximate (isotropic) treatment of cell esds is used for estimating esds involving l.s. planes.

Table S2. Atomic coordinates (x 10^4) and equivalent isotropic displacement parameters ($Å^2$x 10^3) for **2**. U(eq) is defined as the trace of the orthogonalized U^{ij} tensor**.**

	x	y	z	U_{eq}
Ni(1)	1804(1)	1359(1)	7182(1)	12(1)
Cl(1)	3057(1)	1966(1)	8392(1)	19(1)
P(1)	1309(1)	1911(1)	5906(1)	12(1)

P(2)	932(1)	702(1)	8022(1)	12(1)
C(1)	2339(2)	1750(1)	4974(1)	13(1)
C(2)	1905(2)	2079(1)	4132(2)	16(1)
C(3)	2558(2)	1976(1)	3385(2)	18(1)
C(4)	3650(2)	1530(1)	3461(2)	18(1)
C(5)	4085(2)	1198(1)	4279(1)	16(1)
C(6)	3463(2)	1300(1)	5047(1)	13(1)
C(7)	3930(2)	923(1)	5905(1)	12(1)
C(8)	3701(2)	332(1)	5825(2)	14(1)
C(9)	3735(2)	-2(1)	6631(1)	14(1)
C(10)	4003(2)	253(1)	7522(1)	11(1)
C(11)	4448(2)	835(1)	7622(2)	13(1)
C(12)	4426(2)	1167(1)	6827(1)	13(1)
C(13)	3652(2)	-48(1)	8340(1)	12(1)
C(14)	4601(2)	-507(1)	8795(1)	14(1)
C(15)	4306(2)	-790(1)	9560(1)	14(1)
C(16)	3003(2)	-624(1)	9866(1)	15(1)
C(17)	2027(2)	-173(1)	9414(1)	15(1)
C(18)	2323(2)	127(1)	8655(1)	11(1)
C(19)	1756(2)	2696(1)	6082(2)	17(1)
C(20)	866(3)	2974(1)	6737(2)	23(1)
C(21)	3580(3)	2804(1)	6459(2)	23(1)
C(22)	-856(2)	1903(1)	5186(1)	16(1)
C(23)	-1965(3)	1911(1)	5845(2)	22(1)
C(24)	-1281(3)	1389(1)	4514(2)	23(1)
C(25)	84(2)	1004(1)	8958(1)	15(1)
C(26)	-1095(3)	1489(1)	8508(2)	19(1)
C(27)	1323(3)	1214(1)	9873(2)	20(1)
C(28)	-789(2)	262(1)	7266(2)	16(1)
C(29)	-1727(3)	-94(1)	7814(2)	23(1)
C(30)	-221(3)	-130(1)	6591(2)	21(1)

Table S3. Anisotropic displacement parameters ($Å^2 x\ 10^4$) for **2**. The anisotropic displacement factor exponent takes the form: $-2\pi^2[\ h^2 a^{*2} U^{11} + ... + 2\ h\ k\ a^*\ b^*\ U^{12}\ ]$

	U^{11}	U^{22}	U^{33}	U^{23}
Ni(1)	122(1)	129(1)	114(1)	1(1)
Cl(1)	229(3)	172(3)	157(3)	-36(2)
P(1)	115(3)	137(3)	127(3)	9(2)
P(2)	90(3)	139(3)	125(3)	15(2)
C(1)	113(10)	151(11)	126(10)	-6(8)
C(2)	144(11)	165(11)	183(12)	21(9)
C(3)	161(11)	226(12)	137(11)	54(10)
C(4)	174(12)	246(13)	161(12)	-17(10)
C(5)	114(11)	181(12)	191(12)	7(9)
C(6)	77(10)	153(11)	140(10)	-11(9)
C(7)	38(10)	191(11)	157(11)	17(9)
C(8)	103(10)	209(12)	116(11)	-11(9)
C(9)	99(11)	132(11)	183(12)	-1(9)
C(10)	38(9)	169(11)	131(11)	37(9)
C(11)	47(10)	193(11)	118(11)	-21(9)
C(12)	67(10)	144(11)	187(11)	7(9)

C(13)	98(10)	133(10)	110(10)	-25(8)
C(14)	85(10)	155(11)	174(11)	-19(9)
C(15)	117(11)	129(11)	153(11)	13(9)
C(16)	141(11)	169(11)	132(11)	24(9)
C(17)	102(11)	185(11)	164(11)	6(9)
C(18)	80(10)	122(10)	123(11)	-11(8)
C(19)	236(12)	128(11)	165(12)	16(9)
C(20)	326(15)	149(12)	217(13)	9(10)
C(21)	259(13)	186(13)	259(14)	-18(11)
C(22)	137(11)	181(12)	148(11)	48(9)
C(23)	128(12)	320(14)	225(13)	11(12)
C(24)	161(13)	312(14)	214(13)	-26(12)
C(25)	132(11)	162(11)	182(12)	41(9)
C(26)	182(12)	205(13)	218(13)	37(10)
C(27)	237(13)	245(14)	146(12)	-1(10)
C(28)	92(11)	170(11)	189(12)	18(9)
C(29)	172(12)	257(13)	281(14)	0(12)
C(30)	160(12)	226(13)	208(13)	-45(11)

Table S4. Hydrogen coordinates (x 10^4) and isotropic displacement parameters ($Å^2$x 10^3) for **2.**

	x	y	z	U_{iso}
H(1)	1037(19)	1037(7)	6429(13)	16(5)
H(2)	1170(20)	2375(8)	4061(13)	17(5)
H(3)	2226(19)	2202(7)	2823(13)	10(5)
H(4)	4110(20)	1444(8)	2980(13)	16(5)
H(5)	4810(20)	883(8)	4338(12)	9(5)
H(8)	3400(19)	165(7)	5216(12)	4(5)
H(9)	3448(19)	-408(7)	6540(12)	6(5)
H(11)	4811(19)	988(7)	8216(12)	2(5)
H(12)	4773(19)	1575(7)	6889(12)	7(5)
H(14)	5450(20)	-601(7)	8578(13)	13(5)
H(15)	4976(19)	-1104(8)	9865(13)	11(5)
H(16)	2780(19)	-818(7)	10380(13)	9(5)
H(17)	1100(20)	-61(8)	9632(13)	18(5)
H(19)	1288(19)	2879(7)	5431(13)	9(5)
H(20A)	1040(20)	2756(9)	7328(15)	29(6)
H(20B)	-250(20)	3040(8)	6403(15)	27(6)
H(20C)	1280(20)	3367(9)	6948(14)	32(6)
H(21A)	3760(20)	3232(8)	6497(13)	20(5)
H(21B)	4150(20)	2633(9)	6025(15)	33(6)
H(21C)	3990(20)	2638(8)	7104(15)	26(6)
H(22)	-1000(20)	2240(8)	4805(13)	14(5)
H(23A)	-3080(20)	1961(8)	5446(14)	23(6)
H(23B)	-1720(20)	2214(9)	6329(15)	26(6)
H(23C)	-1930(20)	1528(9)	6182(15)	28(6)
H(24A)	-1040(20)	1033(9)	4883(16)	36(7)
H(24B)	-700(20)	1372(9)	4056(15)	30(6)
H(24C)	-2410(20)	1402(8)	4170(14)	24(6)
H(25)	-490(20)	675(8)	9135(13)	17(5)
H(26A)	-1600(20)	1649(8)	9005(13)	17(5)
H(26B)	-1930(20)	1365(8)	7958(14)	17(5)

H(26C)	-550(20)	1809(8)	8300(13)	19(5)
H(27A)	1860(20)	1546(9)	9741(14)	25(6)
H(27B)	2040(20)	896(8)	10205(14)	22(6)
H(27C)	800(20)	1344(9)	10363(15)	33(6)
H(28)	-1511(19)	561(7)	6872(12)	4(5)
H(29A)	-2520(20)	-320(9)	7340(15)	28(6)
H(29B)	-2170(20)	139(8)	8206(15)	25(6)
H(29C)	-1030(20)	-393(9)	8236(15)	26(6)
H(30A)	490(20)	-413(8)	6943(14)	21(6)
H(30B)	250(20)	82(9)	6164(16)	41(7)
H(30C)	-1130(20)	-340(8)	6150(14)	24(6)

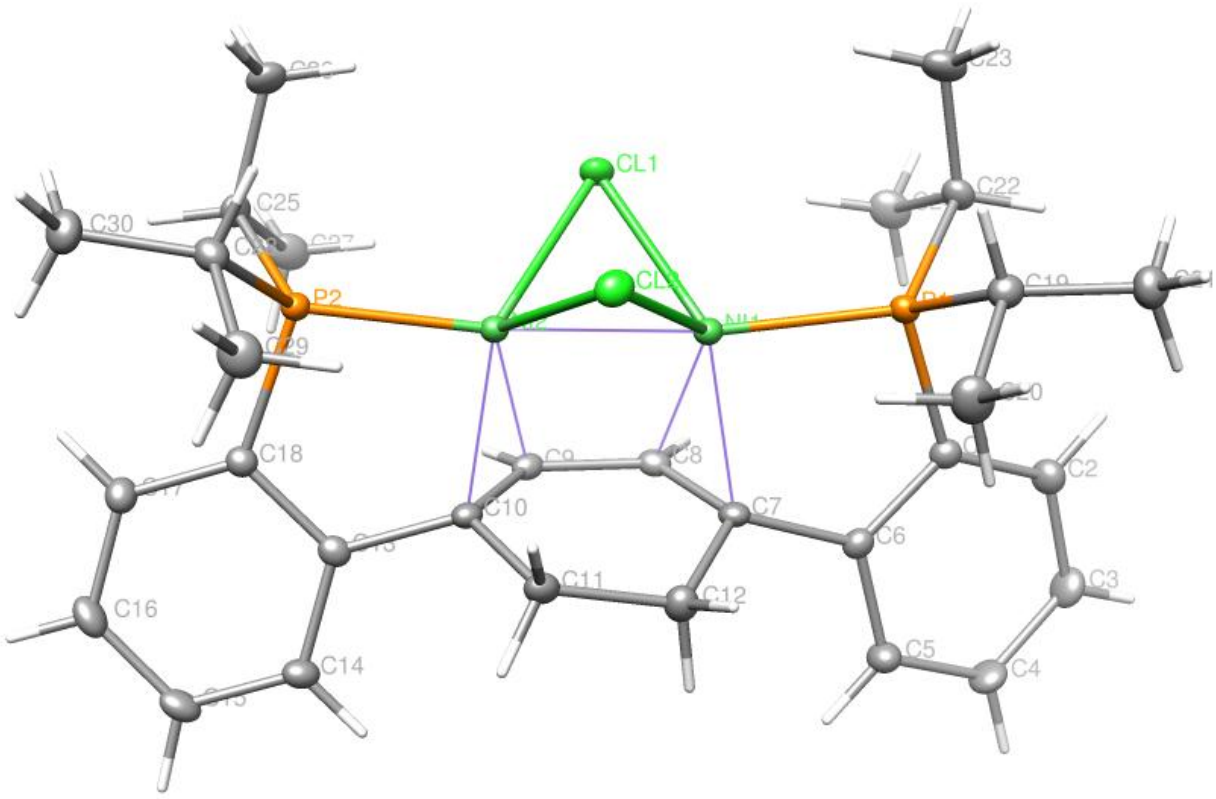

Figure S30. Structural drawing of **3** with 50% thermal probability ellipsoids**.**

Special refinement details for 3. Crystals were mounted on a glass fiber using Paratone oil then placed on the diffractometer under a nitrogen stream at 100K. Refinement of F^2 against ALL reflections. The weighted R-factor (*w*R) and goodness of fit (S) are based on F^2, conventional R-factors (R) are based on F, with F set to zero for negative F^2. The threshold expression of $F^2 > 2\sigma(F^2)$ is used only for calculating R-factors(gt) etc. and is not relevant to the choice of reflections for refinement. R-factors based on F^2 are statistically about twice as large as those based on F, and R-factors based on ALL data will be even larger. All esds (except the esd in the dihedral angle between two l.s. planes) are estimated using the full covariance matrix. The cell esds are taken into account individually in the estimation of esds in distances, angles and torsion angles; correlations between esds in cell parameters are only used when they are defined by crystal symmetry. An approximate (isotropic) treatment of cell esds is used for estimating esds involving l.s. planes.

Table S5. Atomic coordinates (x 10^4) and equivalent isotropic displacement parameters ($Å^2$x 10^3) for **3**. U(eq) is defined as the trace of the orthogonalized U^{ij} tensor.

	x	y	z	U_{eq}
Ni(1)	1605(1)	4223(1)	8031(1)	11(1)
Ni(2)	1134(1)	3455(1)	9039(1)	11(1)
Cl(1)	3215(1)	3871(1)	9207(1)	15(1)
Cl(2)	1151(1)	2847(1)	7793(1)	15(1)
P(1)	2271(1)	4870(1)	7136(1)	12(1)
P(2)	904(1)	2714(1)	10021(1)	11(1)

C(1)	1170(1)	5708(1)	6889(1)	13(1)
C(2)	1337(1)	6414(1)	6498(1)	17(1)
C(3)	384(1)	6991(1)	6316(1)	20(1)
C(4)	-740(1)	6854(1)	6511(1)	20(1)
C(5)	-903(1)	6161(1)	6917(1)	17(1)
C(6)	68(1)	5584(1)	7132(1)	13(1)
C(7)	-26(1)	4888(1)	7667(1)	12(1)
C(8)	577(1)	4982(1)	8521(1)	12(1)
C(9)	225(1)	4492(1)	9112(1)	11(1)
C(10)	-682(1)	3860(1)	8879(1)	12(1)
C(11)	-1462(1)	3773(1)	7988(1)	15(1)
C(12)	-1248(1)	4406(1)	7402(1)	16(1)
C(13)	-1286(1)	3553(1)	9506(1)	12(1)
C(14)	-2517(1)	3790(1)	9496(1)	15(1)
C(15)	-3067(1)	3516(1)	10083(1)	17(1)
C(16)	-2392(1)	3012(1)	10704(1)	18(1)
C(17)	-1162(1)	2786(1)	10735(1)	16(1)
C(18)	-617(1)	3036(1)	10132(1)	12(1)
C(19)	2096(1)	4341(1)	6157(1)	15(1)
C(20)	744(1)	4007(1)	5832(1)	22(1)
C(21)	2460(1)	4836(1)	5510(1)	19(1)
C(22)	3893(1)	5296(1)	7431(1)	15(1)
C(23)	4882(1)	4629(1)	7536(1)	22(1)
C(24)	4092(1)	5776(1)	8218(1)	21(1)
C(25)	2090(1)	2810(1)	11030(1)	16(1)
C(26)	3353(1)	2458(1)	10980(1)	20(1)
C(27)	2233(1)	3690(1)	11280(1)	21(1)
C(28)	721(1)	1625(1)	9807(1)	15(1)
C(29)	-416(1)	1483(1)	9052(1)	21(1)
C(30)	633(1)	1114(1)	10528(1)	21(1)

Table S6. Anisotropic displacement parameters ($Å^2 x\ 10^4$) for **3.** The anisotropic displacement factor exponent takes the form: $-2\pi^2[\ h^2 a^{*2} U^{11} + ... + 2\ h\ k\ a^*\ b^*\ U^{12}\ ]$

	U^{11}	U^{22}	U^{33}	U^{23}
Ni(1)	103(1)	108(1)	123(1)	11(1)
Ni(2)	96(1)	105(1)	118(1)	9(1)
Cl(1)	98(1)	172(2)	162(1)	17(1)
Cl(2)	174(1)	122(1)	151(1)	-22(1)
P(1)	100(1)	123(2)	126(1)	2(1)
P(2)	106(1)	107(2)	130(1)	14(1)
C(1)	122(4)	116(6)	136(4)	1(4)
C(2)	161(5)	156(6)	189(5)	12(4)
C(3)	247(5)	116(6)	222(6)	47(5)
C(4)	209(5)	148(7)	249(6)	64(5)
C(5)	150(4)	163(6)	210(5)	42(5)
C(6)	127(4)	115(6)	128(4)	7(4)
C(7)	96(4)	109(6)	148(5)	10(4)
C(8)	109(4)	90(6)	166(5)	-15(4)
C(9)	117(4)	107(6)	115(4)	-8(4)
C(10)	99(4)	114(6)	130(4)	11(4)
C(11)	116(4)	173(6)	147(5)	11(4)

C(12)	150(4)	173(7)	154(5)	16(4)
C(13)	116(4)	103(6)	135(5)	-27(4)
C(14)	118(4)	151(6)	174(5)	-10(4)
C(15)	126(4)	177(6)	224(5)	-47(5)
C(16)	203(5)	152(6)	226(6)	-29(5)
C(17)	183(5)	120(6)	177(5)	9(4)
C(18)	122(4)	99(6)	148(5)	-9(4)
C(19)	154(4)	137(6)	148(5)	-4(4)
C(20)	209(5)	249(8)	176(6)	-32(5)
C(21)	221(5)	213(7)	156(5)	2(5)
C(22)	117(4)	169(6)	161(5)	-1(4)
C(23)	127(5)	271(8)	238(6)	-25(5)
C(24)	183(5)	206(7)	235(6)	-59(5)
C(25)	140(4)	198(7)	128(5)	42(4)
C(26)	146(5)	217(8)	223(6)	46(5)
C(27)	177(5)	251(8)	182(6)	-42(5)
C(28)	149(4)	113(6)	214(5)	5(4)
C(29)	225(5)	150(7)	237(6)	-38(5)
C(30)	245(6)	128(7)	271(6)	42(5)

Table S7. Hydrogen coordinates (x 10^4) and isotropic displacement parameters ($Å^2$x 10^3) for **3.**

	x	y	z	U_{iso}
H(2)	2099(10)	6513(6)	6374(7)	14(3)
H(3)	507(11)	7444(7)	6075(7)	22(3)
H(4)	-1371(10)	7250(7)	6372(7)	21(3)
H(5)	-1659(9)	6095(6)	7075(6)	13(3)
H(8)	1091(10)	5427(7)	8690(6)	12(3)
H(9)	479(9)	4655(6)	9633(6)	13(3)
H(11A)	-1312(11)	3265(7)	7794(8)	30(4)
H(11B)	-2367(10)	3745(6)	7956(7)	16(3)
H(12A)	-1361(11)	4183(7)	6876(7)	25(3)
H(12B)	-1952(11)	4783(7)	7319(7)	31(4)
H(14)	-2951(10)	4148(7)	9096(7)	14(3)
H(15)	-3882(10)	3699(6)	10065(6)	13(3)
H(16)	-2750(10)	2837(7)	11098(7)	17(3)
H(17)	-699(10)	2477(7)	11165(7)	21(3)
H(19)	2653(10)	3918(7)	6294(6)	15(3)
H(20A)	151(11)	4417(7)	5721(7)	25(3)
H(20B)	540(11)	3667(7)	6214(8)	26(3)
H(20C)	672(11)	3688(7)	5344(8)	28(3)
H(21A)	2345(10)	4524(7)	5023(7)	19(3)
H(21B)	3332(10)	5026(6)	5698(6)	14(3)
H(21C)	1919(11)	5308(7)	5359(7)	25(3)
H(22)	3965(9)	5645(6)	7007(6)	10(3)
H(23A)	5720(12)	4846(7)	7725(7)	29(3)
H(23B)	4839(10)	4330(7)	7037(8)	23(3)
H(23C)	4820(11)	4247(8)	7956(8)	31(4)
H(24A)	4009(11)	5455(8)	8650(8)	32(4)
H(24B)	3512(12)	6205(8)	8136(8)	33(4)
H(24C)	4944(11)	6013(7)	8389(7)	27(3)
H(25)	1801(10)	2534(6)	11414(7)	12(3)

H(26A)	3662(10)	2730(7)	10593(7)	19(3)
H(26B)	3282(10)	1882(8)	10819(7)	22(3)
H(26C)	3999(11)	2491(7)	11504(8)	28(3)
H(27A)	2846(11)	3754(7)	11820(7)	24(3)
H(27B)	1468(11)	3931(7)	11327(7)	19(3)
H(27C)	2524(10)	3986(7)	10887(7)	16(3)
H(28)	1497(9)	1486(6)	9678(6)	8(3)
H(29A)	-509(10)	920(8)	8894(7)	23(3)
H(29B)	-351(11)	1780(7)	8579(7)	24(3)
H(29C)	-1209(11)	1621(7)	9172(7)	22(3)
H(30A)	-152(11)	1210(7)	10647(7)	26(3)
H(30B)	1347(11)	1209(7)	11037(7)	22(3)
H(30C)	616(11)	579(8)	10403(7)	26(4)

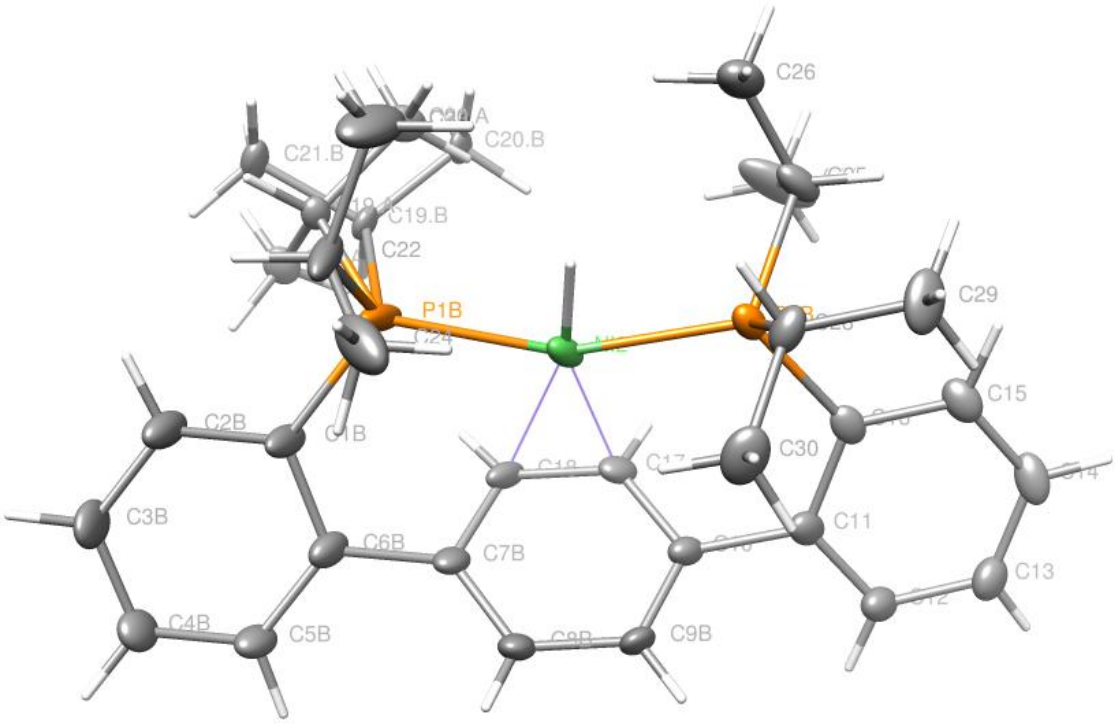

Figure S31. Structural drawing of **5** with 50% thermal probability ellipsoids. Triflate anion cropped for clarity**.**

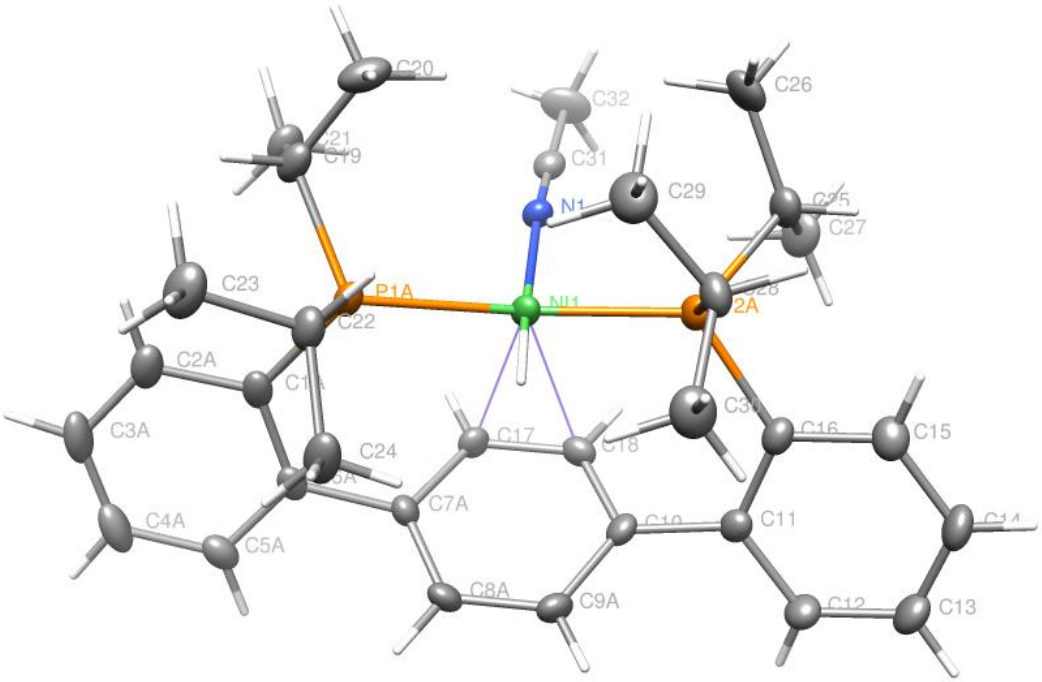

Figure S32. Structural drawing of **5-NCMe** with 50% thermal probability ellipsoids.Triflate anion cropped for clarity.

Special refinement details for 5·OTf + 5-NCMe·OTf. Crystals were mounted on a glass fiber using Paratone oil then placed on the diffractometer under a nitrogen stream at 100K. Hydride atoms on Nickel were located in the electron density difference map and refined without restraint. Refinement of F^2 against ALL reflections. The weighted R-factor (*w*R) and goodness of fit (S) are based on F^2, conventional R-factors (R) are based on F, with F set to zero for negative F^2. The threshold expression of $F^2 > 2\sigma(F^2)$ is used only for calculating R-factors(gt) etc. and is not relevant to the choice of reflections for refinement. R-factors based on F^2 are statistically about twice as large as those based on F, and R-factors based on ALL data will be even larger. All esds (except the esd in the dihedral angle between two l.s. planes) are estimated using the full covariance matrix. The cell esds are taken into account individually in the estimation of esds in distances, angles and torsion angles; correlations between esds in cell parameters are only used when they are defined by crystal symmetry. An approximate (isotropic) treatment of cell esds is used for estimating esds involving l.s. planes.

Table S8. Atomic coordinates (x 10^4) and equivalent isotropic displacement parameters ($Å^2$x 10^3) for **5·OTf** + **5-NCMe·OTf.** U(eq) is defined as the trace of the orthogonalized U^{ij} tensor.

	x	y	z	U_{eq}
Ni(1)	3474(1)	2785(1)	2187(1)	21(1)
P(1A)	2733(1)	2254(1)	2279(1)	24(1)
P(2A)	4099(1)	2411(1)	1806(1)	22(1)
N(1)	3872(1)	3244(2)	3137(1)	22(1)
C(1A)	2188(1)	3186(3)	2089(1)	26(1)
C(2A)	1774(1)	2918(3)	2299(2)	31(1)
C(3A)	1327(1)	3534(3)	2090(2)	34(1)
C(4A)	1278(1)	4383(3)	1666(2)	35(1)
C(5A)	1677(1)	4670(3)	1445(2)	28(1)
C(6A)	2137(1)	4076(3)	1668(1)	23(1)
C(7A)	2563(1)	4371(3)	1423(2)	23(1)
C(8A)	2492(1)	4324(3)	716(2)	25(1)
C(9A)	2917(1)	4338(3)	511(2)	25(1)
C(10A)	3420(1)	4405(3)	1022(2)	23(1)
C(11A)	3873(1)	4158(3)	828(1)	23(1)
C(12A)	3967(1)	4754(3)	313(2)	27(1)
C(13A)	4367(1)	4490(3)	92(2)	30(1)
C(14A)	4673(1)	3622(3)	378(2)	29(1)
C(15A)	4582(1)	3020(3)	884(2)	26(1)
C(16A)	4188(1)	3289(3)	1131(1)	22(1)
C(17A)	3062(1)	4571(3)	1932(2)	24(1)
C(18A)	3489(1)	4588(3)	1731(2)	23(1)
C(19A)	2835(1)	1703(3)	3161(2)	29(1)
C(20A)	3274(2)	892(4)	3359(2)	38(1)
C(21A)	2926(1)	2548(4)	3727(2)	34(1)
C(22A)	2415(1)	1161(3)	1649(2)	28(1)
C(23A)	1998(2)	534(4)	1797(2)	42(1)
C(24A)	2181(1)	1590(4)	894(2)	38(1)
C(25A)	4778(1)	2407(3)	2486(2)	28(1)
C(26A)	4850(1)	1644(4)	3098(2)	34(1)
C(27A)	4954(1)	3522(3)	2734(2)	34(1)
C(28A)	4028(1)	1103(3)	1381(2)	26(1)
C(29A)	3865(2)	263(4)	1800(2)	41(1)

C(30A)	3626(1)	1125(4)	613(2)	36(1)
C(31A)	4121(1)	3570(3)	3674(2)	23(1)
C(32A)	4453(2)	3997(4)	4371(2)	38(1)
Ni(2)	1433(1)	7240(1)	4231(1)	24(1)
P(1B)	2210(1)	7108(1)	4182(1)	41(1)
P(2B)	616(1)	6753(1)	3937(1)	20(1)
C(1B)	2764(1)	7416(3)	4996(2)	38(1)
C(2B)	3274(1)	7251(3)	5031(2)	41(1)
C(3B)	3699(1)	7423(3)	5655(2)	37(1)
C(4B)	3631(1)	7742(3)	6267(2)	32(1)
C(5B)	3131(1)	7899(3)	6244(2)	34(1)
C(6B)	2701(1)	7741(3)	5622(2)	34(1)
C(7B)	2165(1)	7913(3)	5588(1)	29(1)
C(8B)	1984(1)	7494(3)	6075(2)	32(1)
C(9B)	1444(1)	7506(3)	5944(2)	31(1)
C(10B)	1097(1)	7934(3)	5340(1)	25(1)
C(11B)	528(1)	7812(3)	5103(1)	25(1)
C(12B)	259(1)	8189(3)	5512(2)	31(1)
C(13B)	-279(1)	8123(3)	5260(2)	29(1)
C(14B)	-550(1)	7672(3)	4611(2)	26(1)
C(15B)	-286(1)	7277(3)	4204(2)	23(1)
C(16B)	253(1)	7331(2)	4445(1)	18(1)
C(17B)	1281(1)	8456(3)	4858(2)	26(1)
C(18B)	1807(1)	8468(3)	4986(2)	30(1)
C(19B)	2366(2)	7778(5)	3523(3)	16(1)
C(20B)	1862(2)	7863(6)	2866(3)	27(2)
C(21B)	2582(2)	8866(5)	3787(3)	23(2)
C(19C)	2149(2)	8311(7)	3488(3)	20(2)
C(20C)	1611(2)	8407(7)	2898(3)	20(2)
C(21C)	2579(2)	8214(7)	3194(3)	28(2)
C(22B)	2386(1)	5789(4)	3975(2)	62(2)
C(23B)	2062(2)	5444(7)	3218(3)	74(2)
C(24B)	2338(2)	5033(5)	4508(2)	60(2)
C(25B)	207(1)	7032(3)	3006(2)	27(1)
C(26B)	389(1)	6438(4)	2496(2)	40(1)
C(27B)	191(2)	8204(4)	2879(2)	63(2)
C(28B)	580(1)	5332(3)	4078(2)	24(1)
C(29B)	32(1)	4868(4)	3858(2)	32(1)
C(30B)	915(1)	5064(4)	4846(2)	33(1)
S(1)	8740(1)	8964(2)	6521(1)	27(1)
C(63)	8695(3)	7669(8)	6109(5)	27(2)
F(1)	9151(2)	7163(3)	6386(2)	36(1)
F(2)	8344(2)	7071(4)	6214(2)	53(2)
F(3)	8583(2)	7724(5)	5423(2)	28(1)
O(1)	8206(2)	9329(5)	6185(2)	70(2)
O(2)	9301(2)	9408(4)	6405(2)	47(1)
O(3)	8890(3)	8744(8)	7258(4)	32(2)
S(2)	4044(1)	6590(1)	3618(1)	32(1)
C(64)	3878(1)	7965(3)	3382(2)	42(1)
F(4)	3446(1)	8066(2)	2802(1)	64(1)
F(5)	4255(1)	8478(2)	3248(1)	57(1)
F(6)	3807(1)	8492(2)	3904(1)	54(1)

O(4)	3563(1)	6147(2)	3606(1)	45(1)
O(5)	4211(1)	6217(2)	3069(1)	46(1)
O(6)	4450(1)	6668(2)	4314(1)	41(1)
S(3)	8881(1)	9246(3)	6536(2)	17(1)
C(65)	8640(7)	8013(15)	6087(11)	23(4)
F(7)	8155(2)	7765(6)	6031(3)	37(2)
F(8)	8591(4)	8110(8)	5374(5)	27(2)
F(9)	8938(4)	7161(9)	6358(5)	51(3)
O(7)	8956(6)	8966(14)	7265(9)	22(3)
O(8)	8475(3)	9942(6)	6182(3)	25(2)
O(9)	9049(3)	9518(6)	6284(3)	14(2)

Table S9. Anisotropic displacement parameters ($Å^2 x\ 10^4$) for **5·OTf + 5-NCMe·OTf**. The anisotropic displacement factor exponent takes the form: $-2\pi^2[\ h^2a^{*2}U^{11} + ... + 2\ h\ k\ a^*\ b^*\ U^{12}\ ]$

	U^{11}	U^{22}	U^{33}	U^{23}
Ni(1)	125(2)	317(3)	155(2)	36(2)
P(1A)	156(3)	393(7)	147(4)	37(4)
P(2A)	127(3)	310(7)	211(4)	39(4)
N(1)	164(12)	330(20)	173(13)	75(12)
C(1A)	143(14)	480(30)	133(14)	-19(15)
C(2A)	217(16)	520(30)	180(16)	-48(18)
C(3A)	180(16)	610(30)	252(18)	-147(19)
C(4A)	155(16)	560(30)	304(19)	-137(19)
C(5A)	176(15)	410(30)	194(16)	-4(17)
C(6A)	134(14)	400(30)	116(14)	-35(14)
C(7A)	125(13)	350(30)	194(15)	52(15)
C(8A)	150(14)	390(30)	175(16)	64(15)
C(9A)	236(16)	380(30)	147(15)	62(15)
C(10A)	204(15)	310(30)	200(16)	70(15)
C(11A)	150(14)	350(30)	173(15)	32(15)
C(12A)	230(16)	330(30)	263(18)	89(17)
C(13A)	262(17)	410(30)	249(18)	40(17)
C(14A)	236(16)	410(30)	304(18)	3(17)
C(15A)	222(16)	280(30)	300(18)	-19(17)
C(16A)	191(14)	290(30)	190(15)	-5(15)
C(17A)	192(15)	380(30)	136(15)	27(15)
C(18A)	152(14)	310(30)	189(16)	43(15)
C(19A)	216(16)	430(30)	184(16)	33(16)
C(20A)	440(20)	370(30)	280(20)	140(20)
C(21A)	262(18)	550(30)	190(17)	28(18)
C(22A)	187(15)	420(30)	229(17)	2(16)
C(23A)	330(20)	570(40)	330(20)	-20(20)
C(24A)	220(18)	680(40)	199(18)	-60(20)
C(25A)	141(14)	440(30)	251(16)	34(17)
C(26A)	128(16)	490(40)	340(20)	60(20)
C(27A)	207(17)	480(30)	320(20)	-20(20)
C(28A)	149(14)	340(30)	313(18)	24(16)
C(29A)	300(20)	420(40)	510(30)	130(20)
C(30A)	288(19)	480(30)	290(20)	-50(20)
C(31A)	198(15)	270(30)	232(17)	81(15)

C(32A)	340(20)	450(40)	205(19)	-10(20)
Ni(2)	201(2)	374(3)	127(2)	23(2)
P(1B)	301(4)	818(10)	151(4)	-161(5)
P(2B)	170(4)	222(6)	164(4)	51(4)
C(1B)	252(15)	720(30)	206(16)	-192(18)
C(2B)	287(17)	740(40)	260(18)	-200(20)
C(3B)	180(15)	590(30)	367(19)	-117(19)
C(4B)	214(15)	470(30)	262(17)	-77(18)
C(5B)	273(16)	570(30)	182(16)	-115(17)
C(6B)	263(16)	590(30)	226(16)	-115(18)
C(7B)	228(15)	530(30)	129(14)	-100(16)
C(8B)	216(15)	630(30)	108(14)	-16(17)
C(9B)	225(15)	590(30)	132(14)	25(16)
C(10B)	226(15)	380(30)	137(14)	-23(15)
C(11B)	223(14)	340(30)	173(15)	44(15)
C(12B)	267(17)	460(30)	200(17)	-21(17)
C(13B)	268(17)	330(30)	320(19)	14(17)
C(14B)	174(14)	150(20)	393(19)	50(16)
C(15B)	214(15)	150(20)	269(17)	37(15)
C(16B)	180(13)	130(20)	201(14)	70(14)
C(17B)	253(16)	390(30)	129(15)	-59(16)
C(18B)	278(17)	510(30)	146(15)	-86(16)
C(19B)	140(30)	180(40)	160(30)	40(30)
C(20B)	320(30)	310(50)	190(30)	60(30)
C(21B)	220(30)	250(50)	210(30)	80(30)
C(19C)	140(30)	320(60)	190(40)	20(40)
C(20C)	110(30)	340(60)	180(30)	40(30)
C(21C)	160(30)	480(70)	250(40)	110(40)
C(22B)	232(18)	1250(50)	470(20)	-590(30)
C(23B)	680(30)	1230(70)	440(30)	-520(30)
C(24B)	270(20)	910(50)	460(30)	-290(30)
C(25B)	255(16)	300(30)	175(15)	35(15)
C(26B)	340(20)	640(40)	196(19)	-20(20)
C(27B)	820(40)	490(40)	250(20)	120(20)
C(28B)	222(15)	240(30)	310(18)	48(16)
C(29B)	292(19)	170(30)	550(30)	-20(20)
C(30B)	340(20)	290(30)	410(20)	180(20)
S(1)	280(10)	295(14)	218(7)	-20(7)
C(63)	200(30)	330(70)	280(40)	-150(50)
F(1)	400(20)	260(30)	370(19)	-27(15)
F(2)	530(20)	750(40)	440(20)	-270(20)
F(3)	292(18)	380(40)	157(17)	-40(20)
O(1)	430(30)	970(60)	460(30)	-230(30)
O(2)	530(30)	430(40)	560(30)	-90(20)
O(3)	270(30)	490(60)	190(20)	-110(30)
S(2)	250(4)	451(8)	279(4)	21(4)
C(64)	390(20)	570(30)	206(17)	-13(19)
F(4)	639(14)	800(20)	256(11)	-32(12)
F(5)	714(15)	500(20)	515(15)	209(12)
F(6)	522(13)	700(20)	307(12)	-119(11)
O(4)	248(12)	730(20)	399(15)	-45(14)
O(5)	573(16)	460(20)	507(16)	-77(14)

O(6)	310(12)	490(20)	321(13)	105(12)

Table S10. Hydrogen coordinates (x 10^4) and isotropic displacement parameters ($Å^2$x 10^3) for **5·OTf + 5-NCMe·OTf**.

	x	y	z	U_{iso}
H(1)	3218(9)	2420(20)	1520(13)	26(8)
H(2A)	1818(9)	2360(20)	2589(12)	6(7)
H(3A)	1081(10)	3340(20)	2279(13)	26(8)
H(4A)	987(9)	4840(20)	1520(13)	14(8)
H(5A)	1648(9)	5300(20)	1178(12)	6(7)
H(8A)	2153(10)	4200(20)	353(14)	26(8)
H(9A)	2869(9)	4230(20)	20(13)	16(7)
H(12A)	3801(10)	5370(20)	160(14)	22(9)
H(13A)	4412(10)	4850(20)	-265(14)	25(8)
H(14A)	4927(10)	3380(20)	229(13)	28(9)
H(15A)	4774(9)	2420(20)	1066(13)	18(8)
H(17A)	3109(9)	4740(20)	2405(14)	23(8)
H(18A)	3804(9)	4780(20)	2075(13)	18(8)
H(19A)	2538(9)	1340(20)	3122(12)	12(7)
H(20A)	3625(13)	1250(30)	3431(17)	63(12)
H(20B)	3224(12)	270(30)	3018(18)	62(13)
H(20C)	3310(11)	610(30)	3780(16)	42(10)
H(21A)	3017(12)	2210(30)	4221(19)	69(12)
H(21B)	2634(12)	3060(30)	3657(15)	47(11)
H(21C)	3204(10)	2940(20)	3785(13)	23(8)
H(22A)	2735(9)	630(20)	1723(12)	8(7)
H(23A)	1694(14)	960(30)	1780(19)	79(15)
H(23B)	2129(13)	170(30)	2250(20)	79(14)
H(23C)	1883(11)	-120(30)	1455(16)	42(10)
H(24A)	2063(11)	980(30)	562(16)	37(10)
H(24B)	2428(10)	1930(20)	762(13)	21(8)
H(24C)	1884(12)	2030(30)	813(16)	48(11)
H(25A)	4988(9)	2140(20)	2255(13)	22(8)
H(26A)	5182(12)	1740(30)	3473(17)	56(11)
H(26B)	4831(10)	890(30)	2955(15)	25(10)
H(26C)	4590(10)	1710(20)	3322(13)	25(8)
H(27A)	4716(10)	3870(20)	2960(14)	32(9)
H(27B)	4938(11)	4030(30)	2367(17)	49(11)
H(27C)	5289(12)	3510(30)	3090(16)	50(11)
H(28A)	4372(10)	820(20)	1337(14)	34(9)
H(29A)	3525(14)	460(30)	1808(18)	77(14)
H(29B)	4115(14)	90(30)	2290(20)	80(14)
H(29C)	3826(12)	-460(30)	1576(18)	55(13)
H(30A)	3603(11)	390(30)	412(17)	50(12)
H(30B)	3692(11)	1590(30)	298(15)	37(10)
H(30C)	3278(10)	1350(20)	618(13)	26(8)
H(32A)	4678(14)	3490(30)	4555(19)	62(14)
H(32B)	4298(18)	4090(40)	4650(30)	130(20)
H(32C)	4542(19)	4670(50)	4280(30)	140(30)
H(18B)	1941(10)	8910(30)	4743(15)	35(9)
H(19B)	2629	7361	3406	24
H(20D)	1729	7155	2703	41

H(20E)	1931	8234	2489	41
H(20F)	1603	8257	2987	41
H(21D)	2881	8799	4237	35
H(21E)	2312	9294	3859	35
H(21F)	2692	9208	3435	35
H(19C)	2213	8982	3767	30
H(20G)	1526	7749	2625	30
H(20H)	1611	8993	2583	30
H(20I)	1351	8540	3106	30
H(21G)	2526	7570	2908	42
H(21H)	2918	8180	3588	42
H(21I)	2570	8829	2897	42
H(2)	1345(10)	6440(20)	3766(14)	38(9)
H(2B)	3350(9)	7040(20)	4633(13)	23(8)
H(3B)	4038(9)	7310(20)	5665(12)	17(7)
H(4B)	3933(10)	7850(20)	6703(14)	36(9)
H(5B)	3096(9)	8150(20)	6672(13)	14(7)
H(8B)	2196(10)	7040(20)	6458(14)	33(9)
H(9B)	1332(9)	7200(20)	6261(13)	25(8)
H(12B)	448(10)	8550(20)	5933(14)	25(8)
H(13B)	-414(9)	8380(20)	5529(13)	18(8)
H(14B)	-918(11)	7640(30)	4427(15)	41(9)
H(15B)	-487(9)	6870(20)	3754(13)	23(8)
H(17B)	1061(10)	8950(20)	4523(14)	27(9)
H(22B)	2755(12)	5790(30)	4048(16)	58(11)
H(23D)	2160(14)	4820(30)	3150(20)	54(16)
H(23E)	2127(17)	5870(40)	2890(20)	110(20)
H(23F)	1662(14)	5390(30)	3149(18)	75(13)
H(24D)	2005(12)	4940(30)	4481(17)	48(11)
H(24E)	2520(14)	5270(30)	4990(20)	88(15)
H(24F)	2419(13)	4310(30)	4479(19)	61(14)
H(25B)	-131(11)	6740(30)	2934(15)	45(10)
H(26D)	167(11)	6560(20)	2021(15)	32(9)
H(26E)	424(12)	5650(30)	2567(18)	57(14)
H(26F)	727(12)	6700(30)	2516(16)	52(11)
H(27D)	499(12)	8570(30)	2978(16)	41(11)
H(27E)	51(13)	8610(30)	3159(19)	62(15)
H(27F)	-48(13)	8340(30)	2374(19)	69(12)
H(28B)	719(9)	5070(20)	3775(13)	12(7)
H(29D)	45(10)	4140(30)	3884(14)	19(9)
H(29E)	-200(12)	5060(30)	3365(18)	61(12)
H(29F)	-130(10)	5160(20)	4157(14)	33(9)
H(30D)	789(10)	5320(20)	5212(14)	26(8)
H(30E)	1245(11)	5350(20)	4967(14)	28(9)
H(30F)	936(11)	4350(30)	4898(16)	32(11)

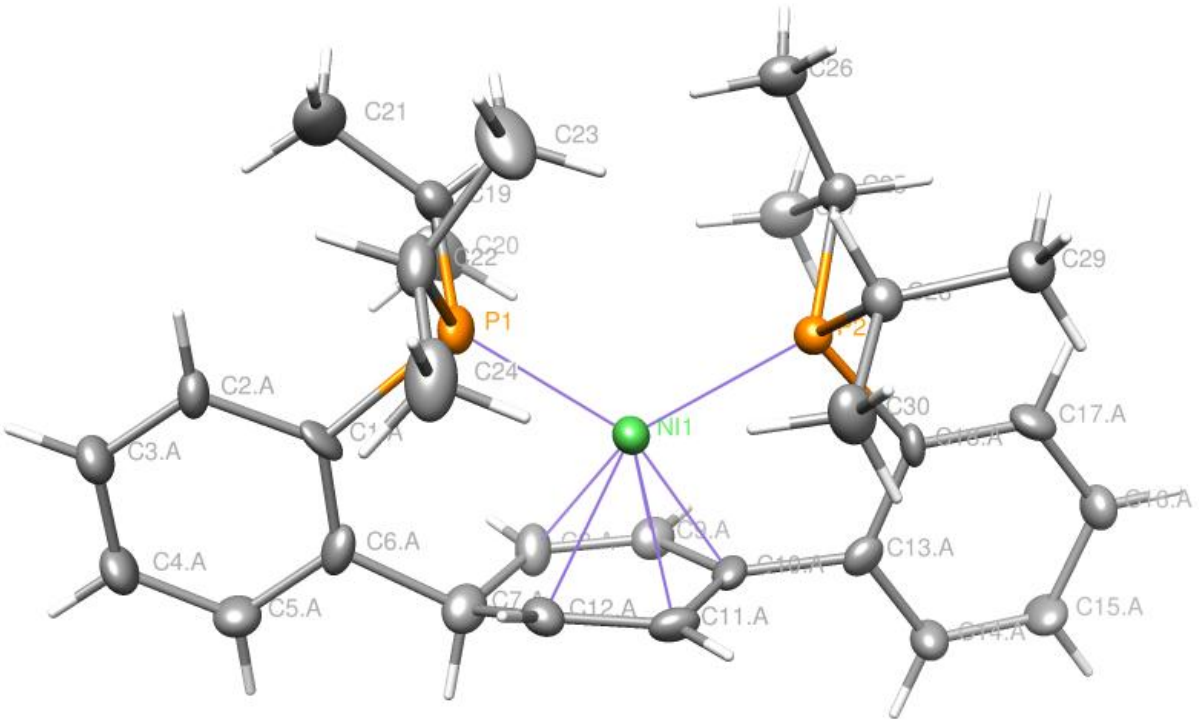

Figure S33. Structural drawing of major enantiomer (70.6%) in crystal of **7·BAr$_{F24}$** with 50% thermal probability ellipsoids**.** The nickel atom is in the proximal half of the molecule from this view.

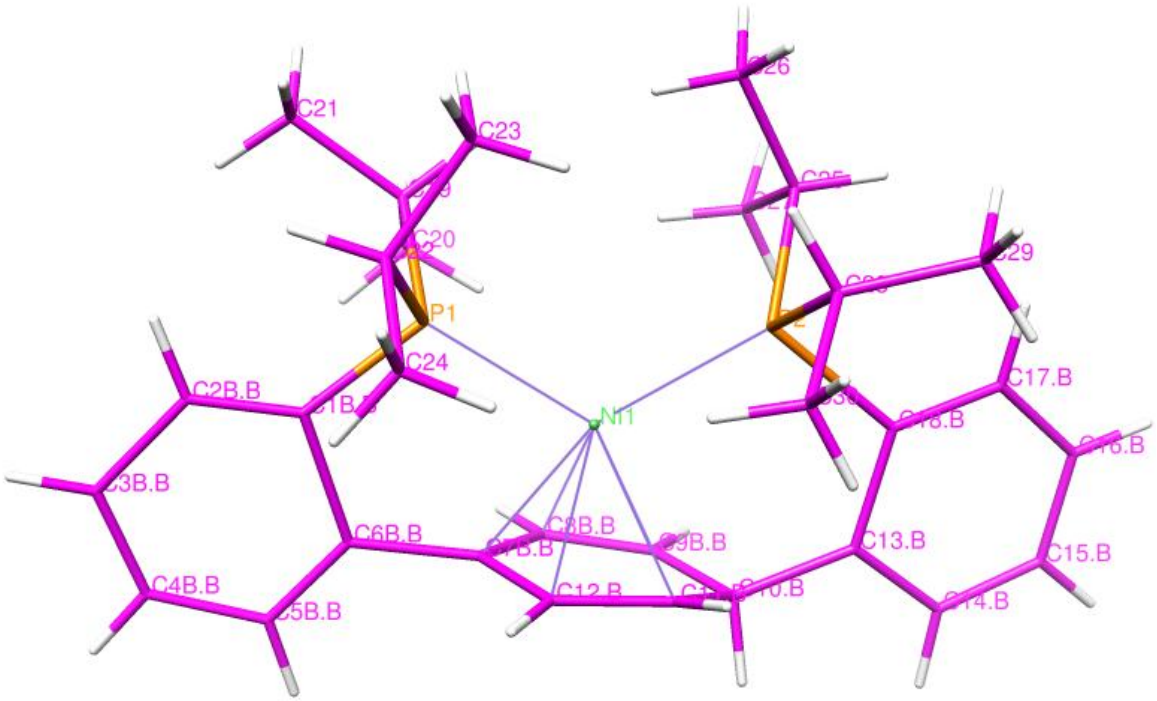

Figure S34. Structural drawing of minor enantiomer (29.4%) in crystal of **7·BAr$_{F24}$.** The nickel atom is in the proximal half of the molecule from this view.

Special refinement details for 7·BAr$_{F24}$. Crystals were mounted on a glass fiber using Paratone oil then placed on the

diffractometer under a nitrogen stream at 100K. All hydrogen atoms were located in the difference map and refined as riding atoms. There is disorder present in C(1)-C(18) and two CF_3 groups. No restraints were used in modeling the disorder, minor components were refined isotropically. Refinement of F^2 against ALL reflections. The weighted R-factor (*w*R) and goodness of fit (S) are based on F^2, conventional R-factors (R) are based on F, with F set to zero for negative F^2. The threshold expression of $F^2 > 2\sigma(F^2)$ is used only for calculating R-factors(gt) etc. and is not relevant to the choice of reflections for refinement. R-factors based on F^2 are statistically about twice as large as those based on F, and R-factors based on ALL data will be even larger. All esds (except the esd in the dihedral angle between two l.s. planes) are estimated using the full covariance matrix. The cell esds are taken into account individually in the estimation of esds in distances, angles and torsion angles; correlations between esds in cell parameters are only used when they are defined by crystal symmetry. An approximate (isotropic) treatment of cell esds is used for estimating esds involving l.s. planes.

Table S11. Atomic coordinates (x 104) and equivalent isotropic displacement parameters ($Å^2 x\ 10^3$) for **7·BAr$_{F24}$.** U(eq) is defined as the trace of the orthogonalized U^{ij} tensor.

	x	y	z	U_{eq}
Ni(1)	2520(1)	7315(1)	3173(1)	22(1)
P(1)	3405(1)	6876(1)	2839(1)	26(1)
P(2)	2812(1)	8307(1)	3907(1)	20(1)
C(1)	2992(6)	6001(5)	2278(6)	23(2)
C(2)	3446(5)	5665(4)	1927(4)	25(1)
C(3)	3246(3)	5002(2)	1595(2)	32(1)
C(4)	2592(3)	4648(2)	1585(2)	34(1)
C(5)	2127(2)	4976(2)	1878(2)	32(1)
C(6)	2344(3)	5683(3)	2215(2)	26(1)
C(7)	1787(2)	6031(2)	2501(2)	28(1)
C(8)	2099(3)	6020(2)	3341(2)	27(1)
C(9)	1969(2)	6561(2)	3752(2)	24(1)
C(10)	1567(2)	7232(2)	3389(2)	22(1)
C(11)	1298(3)	7308(3)	2590(3)	24(1)
C(12)	1553(3)	6799(2)	2217(3)	22(1)
C(13)	1453(3)	7795(3)	3891(3)	21(1)
C(14)	831(2)	7753(2)	4088(2)	27(1)
C(15)	795(2)	8240(2)	4623(2)	30(1)
C(16)	1376(2)	8759(2)	4966(2)	26(1)
C(17)	1991(3)	8789(3)	4756(3)	26(1)
C(18)	2035(5)	8309(3)	4212(4)	18(1)
C(1B)	3068(15)	6110(12)	2322(14)	18(4)
C(2B)	3347(13)	5635(12)	2024(12)	40(6)
C(3B)	2966(7)	4921(7)	1637(7)	34(3)
C(4B)	2278(8)	4759(7)	1661(7)	37(3)
C(5B)	1911(6)	5202(5)	1988(5)	34(3)
C(6B)	2240(7)	5843(6)	2318(6)	15(3)
C(7B)	1933(5)	6379(5)	2684(5)	21(2)
C(8B)	2037(7)	6229(6)	3470(7)	21(3)
C(9B)	1736(6)	6684(6)	3793(6)	25(3)
C(10B)	1259(6)	7327(4)	3439(4)	25(2)
C(11B)	1279(8)	7497(8)	2712(8)	28(4)
C(12B)	1489(8)	7001(7)	2319(8)	25(3)
C(13B)	1353(9)	7938(7)	3972(8)	21(3)
C(14B)	838(6)	8009(6)	4319(6)	24(3)

C(15B)	971(6)	8510(6)	4865(6)	34(3)
C(16B)	1598(6)	8978(5)	5112(6)	29(3)
C(17B)	2123(7)	8945(6)	4816(7)	7(2)
C(18B)	2029(11)	8455(8)	4266(11)	6(3)
C(19)	4345(1)	6589(1)	3642(1)	32(1)
C(20)	4189(1)	6001(1)	4119(1)	43(1)
C(21)	5000(1)	6338(1)	3432(1)	54(1)
C(22)	3653(1)	7435(1)	2192(1)	33(1)
C(23)	4162(1)	8102(1)	2607(1)	51(1)
C(24)	2894(1)	7676(1)	1506(1)	43(1)
C(25)	3724(1)	8376(1)	4811(1)	22(1)
C(26)	4447(1)	8539(1)	4683(1)	28(1)
C(27)	3830(1)	7666(1)	5262(1)	34(1)
C(28)	2764(1)	9180(1)	3407(1)	22(1)
C(29)	2710(1)	9870(1)	3829(1)	30(1)
C(30)	2100(1)	9170(1)	2592(1)	32(1)
B(1)	2035(1)	1970(1)	1496(1)	21(1)
F(1)	4262(1)	446(1)	3843(1)	37(1)
F(2)	5037(1)	982(1)	3467(1)	36(1)
F(3)	4875(1)	-184(1)	3344(1)	50(1)
F(4)	3487(1)	-775(1)	683(1)	61(1)
F(5)	3325(1)	208(1)	56(1)	60(1)
F(6)	2331(1)	-323(1)	37(1)	91(1)
F(4B)	2581(6)	-754(5)	470(5)	36(3)
F(5B)	3681(8)	-460(7)	588(8)	60(4)
F(6B)	2749(7)	111(5)	-100(6)	36(3)
F(7)	4485(1)	3131(1)	4078(2)	91(1)
F(8)	4234(2)	3856(2)	3161(1)	129(1)
F(9)	4027(1)	4166(1)	4091(1)	101(1)
F(7B)	4325(9)	3561(10)	4303(8)	92(5)
F(8B)	4105(7)	4228(6)	3435(8)	48(4)
F(9B)	4591(5)	3305(5)	3393(6)	37(3)
F(10)	1001(1)	2723(1)	3619(1)	80(1)
F(11)	1456(1)	3811(1)	3946(1)	80(1)
F(12)	572(1)	3591(1)	2807(1)	51(1)
F(13)	3862(1)	3743(1)	370(1)	65(1)
F(14)	3867(1)	2581(1)	188(1)	58(1)
F(15)	3221(1)	3297(1)	-747(1)	50(1)
F(16)	588(1)	4396(1)	111(1)	38(1)
F(17)	79(1)	3692(1)	-873(1)	38(1)
F(18)	858(1)	4572(1)	-839(1)	39(1)
F(19)	637(1)	78(1)	2600(1)	51(1)
F(20)	-12(1)	1058(1)	2551(1)	40(1)
F(21)	-604(1)	141(1)	1832(1)	47(1)
F(22)	-290(1)	977(1)	-1072(1)	49(1)
F(23)	-1175(1)	562(1)	-794(1)	66(1)
F(24)	-1027(1)	1718(1)	-858(1)	73(1)
C(41)	2689(1)	1312(1)	1682(1)	19(1)
C(42)	3296(1)	1137(1)	2399(1)	21(1)
C(43)	3822(1)	560(1)	2506(1)	20(1)
C(44)	3759(1)	131(1)	1901(1)	22(1)
C(45)	3152(1)	282(1)	1183(1)	22(1)
C(46)	2638(1)	857(1)	1080(1)	23(1)
C(47)	4486(1)	446(1)	3279(1)	28(1)

C(48)	3068(1)	-160(1)	509(1)	33(1)
C(49)	2228(1)	2503(1)	2239(1)	24(1)
C(50)	2973(1)	2834(1)	2622(1)	30(1)
C(51)	3156(1)	3307(1)	3235(1)	35(1)
C(52)	2603(1)	3476(1)	3497(1)	42(1)
C(53)	1859(1)	3176(1)	3122(1)	35(1)
C(54)	1682(1)	2702(1)	2506(1)	29(1)
C(55)	3970(2)	3611(1)	3628(2)	54(1)
C(56)	1234(1)	3328(1)	3378(1)	46(1)
C(57)	2053(1)	2527(1)	844(1)	20(1)
C(58)	2684(1)	2586(1)	654(1)	24(1)
C(59)	2695(1)	3101(1)	135(1)	24(1)
C(60)	2067(1)	3580(1)	-228(1)	24(1)
C(61)	1440(1)	3539(1)	-50(1)	20(1)
C(62)	1436(1)	3031(1)	476(1)	20(1)
C(63)	3402(1)	3176(1)	-15(1)	37(1)
C(64)	749(1)	4050(1)	-413(1)	28(1)
C(65)	1186(1)	1553(1)	1209(1)	20(1)
C(66)	980(1)	1195(1)	1732(1)	22(1)
C(67)	268(1)	832(1)	1508(1)	23(1)
C(68)	-267(1)	788(1)	744(1)	25(1)
C(69)	-72(1)	1111(1)	212(1)	22(1)
C(70)	637(1)	1487(1)	440(1)	21(1)
C(71)	74(1)	520(1)	2114(1)	32(1)
C(72)	-639(1)	1092(1)	-616(1)	33(1)

Table S12. Anisotropic displacement parameters ($Å^2 x\ 10^4$) for **7·BAr$_{F24}$.** The anisotropic displacement factor exponent takes the form: $-2\pi^2[\ h^2a^{*2}U^{11} + ... + 2\ h\ k\ a^*\ b^*\ U^{12}\ ]$

	U^{11}	U^{22}	U^{33}	U^{23}
Ni(1)	195(1)	227(1)	252(1)	-71(1)
P(1)	301(3)	191(3)	339(3)	-54(2)
P(2)	197(3)	217(3)	213(3)	-38(2)
C(1)	250(30)	120(30)	230(30)	-70(20)
C(2)	280(30)	270(20)	240(30)	-86(18)
C(3)	330(30)	310(20)	350(20)	-156(15)
C(4)	360(30)	320(20)	380(20)	-180(15)
C(5)	250(20)	400(30)	350(20)	-83(18)
C(6)	280(20)	330(20)	220(20)	-19(17)
C(7)	309(19)	240(20)	340(20)	19(16)
C(8)	380(20)	210(20)	310(20)	-21(18)
C(9)	250(20)	210(20)	280(20)	37(15)
C(10)	156(17)	213(16)	333(19)	-74(14)
C(11)	129(18)	300(30)	250(20)	30(20)
C(12)	210(20)	250(20)	220(20)	-59(19)
C(13)	170(20)	230(20)	240(20)	41(19)
C(14)	236(17)	248(19)	370(20)	-103(17)
C(15)	234(19)	340(20)	410(30)	-90(20)
C(16)	290(20)	240(20)	290(20)	-77(17)
C(17)	230(30)	220(30)	300(20)	-60(20)
C(18)	240(20)	140(30)	180(20)	-50(20)
C(19)	264(12)	314(12)	370(13)	-171(10)

C(20)	402(13)	349(13)	364(13)	-19(11)
C(21)	270(13)	686(17)	572(16)	-257(13)
C(22)	460(13)	264(11)	431(13)	-76(10)
C(23)	782(17)	368(13)	636(16)	-146(12)
C(24)	694(16)	329(12)	452(14)	36(11)
C(25)	190(10)	262(11)	220(10)	-52(9)
C(26)	204(11)	328(11)	294(11)	-18(9)
C(27)	302(11)	421(12)	296(12)	45(10)
C(28)	223(10)	209(10)	240(11)	-33(8)
C(29)	307(12)	243(11)	358(12)	-48(9)
C(30)	355(12)	251(11)	301(12)	-14(9)
B(1)	204(12)	232(12)	166(12)	-13(10)
F(1)	353(7)	481(7)	247(6)	95(5)
F(2)	246(6)	453(7)	317(7)	-37(5)
F(3)	475(8)	381(7)	420(8)	-10(6)
F(4)	1209(17)	278(10)	406(10)	57(8)
F(5)	1143(18)	431(10)	465(10)	-74(8)
F(6)	362(11)	1370(20)	877(16)	-902(16)
F(7)	306(10)	413(11)	1450(20)	85(13)
F(8)	894(19)	2200(40)	545(16)	-255(19)
F(9)	589(12)	617(13)	1320(20)	-726(13)
F(10)	1153(12)	671(10)	977(11)	324(9)
F(11)	748(10)	1053(12)	461(9)	-366(8)
F(12)	538(8)	536(8)	406(8)	-32(6)
F(13)	446(8)	670(9)	1001(11)	-305(8)
F(14)	476(8)	519(8)	982(11)	322(8)
F(15)	617(8)	469(8)	650(9)	117(7)
F(16)	367(7)	343(7)	431(7)	-12(6)
F(17)	225(6)	373(7)	411(7)	25(6)
F(18)	357(7)	305(6)	463(7)	166(6)
F(19)	557(8)	578(8)	570(8)	362(7)
F(20)	485(7)	404(7)	448(7)	55(6)
F(21)	489(8)	395(7)	651(9)	91(6)
F(22)	431(8)	698(9)	286(7)	-51(6)
F(23)	528(8)	881(10)	408(8)	-44(7)
F(24)	751(10)	562(9)	408(8)	-76(7)
C(41)	181(10)	184(10)	181(10)	-10(8)
C(42)	216(10)	209(10)	216(11)	-36(8)
C(43)	194(10)	190(10)	204(11)	28(8)
C(44)	232(11)	172(10)	299(12)	18(9)
C(45)	263(11)	172(10)	234(11)	-27(8)
C(46)	218(10)	230(10)	200(10)	1(9)
C(47)	268(12)	261(11)	290(12)	5(9)
C(48)	360(14)	318(13)	311(13)	6(11)
C(49)	276(11)	209(11)	180(10)	38(8)
C(50)	309(12)	225(11)	256(11)	10(9)
C(51)	343(13)	228(11)	247(12)	-15(9)
C(52)	545(16)	263(12)	265(12)	-62(10)
C(53)	442(14)	314(12)	208(11)	-15(10)
C(54)	327(12)	259(11)	213(11)	-12(9)
C(55)	624(19)	354(15)	411(17)	-76(13)
C(56)	631(17)	413(15)	359(14)	-39(12)
C(57)	180(10)	206(10)	179(10)	-63(8)
C(58)	193(11)	201(10)	289(11)	-11(9)

C(59)	238(11)	236(11)	295(11)	-17(9)
C(60)	286(12)	189(10)	261(11)	-12(9)
C(61)	202(10)	165(10)	203(10)	-35(8)
C(62)	184(10)	198(10)	222(10)	-58(8)
C(63)	341(13)	306(13)	545(15)	36(12)
C(64)	262(12)	249(11)	283(12)	16(10)
C(65)	221(10)	172(10)	188(10)	-8(8)
C(66)	253(11)	216(10)	190(10)	13(8)
C(67)	255(11)	190(10)	296(12)	62(9)
C(68)	178(10)	195(10)	369(12)	4(9)
C(69)	199(11)	196(10)	228(11)	13(8)
C(70)	244(11)	190(10)	226(11)	27(8)
C(71)	297(12)	293(12)	398(13)	73(11)
C(72)	240(12)	331(13)	345(13)	-15(10)

References

(1) Velian, A.; Lin, S.; Miller, A. J. M.; Day, M. W.; Agapie, T. *J. Am. Chem. Soc.* **2010**, *132*, 6296.

(2) Brookhart, M.; Grant, B.; Volpe, A. F. *Organometallics* **1992**, *11*, 3920.

(3) Pangborn, A. B.; Giardello, M. A.; Grubbs, R. H.; Rosen, R. K.; Timmers, F. J. *Organometallics* **1996**, *15*, 1518.

(4) Fulmer, G. R.; Miller, A. J. M.; Sherden, N. H.; Gottlieb, H. E.; Nudelman, A.; Stoltz, B. M.; Bercaw, J. E.; Goldberg, K. I. *Organometallics* **2010**, *29*, 2176.

(5) Lulinski, P.; Skulski, L. *Bull. Chem. Soc. Jpn.* **2000**, *73*, 951.